Title
Cross-climate analysis of energy flexibility in high thermal mass radiant systems

Journal
Science and Technology for the Built Environment

ISSN
2374-4731 2374-474X

Authors
Lv, Guoquan
Duarte Roa, Carlos
Zhao, Kang
et al.

Publication Date
2026-03-09

DOI
10.1080/23744731.2026.2631318

Data Availability
The data associated with this publication are available upon request.

Science and Technology for the Built Environment

ISSN: 2374-4731 (Print) 2374-474X (Online) Journal homepage: www.tandfonline.com/journals/uhvc21

Cross-climate analysis of energy flexibility in high thermal mass radiant systems

Guoquan Lv, Carlos Duarte Roa, Kang Zhao & Jian Ge

To cite this article: Guoquan Lv, Carlos Duarte Roa, Kang Zhao & Jian Ge (09 Mar 2026): Cross-climate analysis of energy flexibility in high thermal mass radiant systems, Science and Technology for the Built Environment, DOI: 10.1080/23744731.2026.2631318

To link to this article: https://doi.org/10.1080/23744731.2026.2631318

Published online: 09 Mar 2026.

Science and Technology for the Built Environment, (2026) **0**, 1–26

ISSN: 2374-4731 print / 2374-474X online
DOI: 10.1080/23744731.2026.2631318

Cross-climate analysis of energy flexibility in high thermal mass radiant systems

GUOQUAN LV[1,2], CARLOS DUARTE ROA[2]*, KANG ZHAO[1], and JIAN GE[1]

[1]*Department of Architecture, Zhejiang University, Hangzhou, 310058, China*
[2]*Center for the Built Environment, UC Berkeley, Berkeley, CA, USA*

High thermal mass radiant systems have strong potential for energy flexibility, but key parameter relationships remain unclear. This study conducts a comprehensive parameter sensitivity analysis of thermally activated building systems (TABS) and embedded surface systems (ESS) using hundreds of thousands of simulations. Two representative cases, Hangzhou, China (humid subtropical) and San Francisco, California, USA (marine), are analyzed in depth, followed by cross-climate testing in eight additional cities spanning hot to mild climates. Results show that start/stop is the primary driver of load shifting potential, while start time has little effect on cooling energy supply. For floor ESS, however, operation duration is critical: Extending operation from 8 to 24 h increases daily cooling supply by 25.9% in Hangzhou and by 35.4% in San Francisco, compared to only 5–9% in other terminal types. Using San Francisco as an example, a comparison of fixed nighttime precooling and flexible scheduling reveals key design levers, such as window-to-wall ratios and optimal orientations, that strengthen energy flexibility. Overall, the findings support a two-stage optimization: first, tuning operation timing and durations to maximize load shifting without excess cooling, and second, refining design parameters to enhance flexibility. These insights provide guidance for designing grid-interactive radiant cooling systems.

Introduction

As global energy systems transition toward decarbonization, the large-scale integration of renewable energy sources—such as wind and solar—is rapidly reshaping the electricity supply–demand landscape. In this context, demand-side flexibility has emerged as a key strategy to ensure system balance and reduce the integration cost of renewables (Heptonstall and Gross 2020; O'Shaughnessy et al. 2022). Simultaneously, the global stock of room air conditioners has surpassed 2 billion units, continuously driving electricity demand and intensifying peak load stress (IEA 2023). According to the U.S. Department of Energy, HVAC (heating, ventilation, and air conditioning) loads account for approximately 42% of total energy consumption in residential and commercial buildings and contribute around 44% of peak electricity demand during 14:00–20:00 (Neukomm et al. 2019). Similarly, in Zhejiang Province, China, cooling loads during summer peak hours can account for up to 40% of total electricity demand (China Energy News 2023). Against this backdrop, HVAC systems are increasingly recognized as a key enabler of building energy flexibility, owing to their ability to exploit building thermal inertia and occupants' tolerance for thermal comfort variation (Vivian et al. 2020; Tang et al. 2021; Lv et al. 2024).

The amount of building thermal mass that can be activated is a crucial factor determining the effectiveness of flexibility strategies without compromising indoor comfort (Braun 1990; Gallardo and Berardi 2022). According to research by the Pacific Northwest National Laboratory, thermal inertia is more sensitive to HVAC system type than to floor area or location (Huang et al. 2021). Compared with typical convective cooling systems, high thermal mass radiant systems can directly activate structural mass (ISO 2012; Olsthoorn et al. 2017). Ahn et al. (2021) found that under the same demand response strategy, concrete radiant floor systems can reduce peak cooling load by 20–34% compared to all-air systems, mainly due to their thermal storage capability. Prior studies revealed that conventional all-air systems typically utilize only 7.8%–18.7% of the available

Received August 26, 2025; accepted January 16, 2026
Guoquan Lv, PhD, is a Postdoctoral Scholar. **Carlos Duarte Roa, PhD**, Associate Member ASHRAE, is an Assistant Professional Researcher. **Kang Zhao, PhD**, is an Associate Professor. **Jian Ge, PhD**, is a Professor.
*Corresponding author e-mail: cduarte@berkeley.edu

building thermal mass, while radiant floor systems can increase this proportion to 38.9%–48.3% (Xu et al. 2024).

Extensive experimental and empirical studies have confirmed the strong potential of high thermal mass systems in reducing peak loads and shifting cooling demand (Olesen 2008; Olsthoorn et al. 2017). For instance, a study on a residential building equipped with high thermal mass in a hot-dry climate showed that daily HVAC peak loads could be reduced by 47% to 88%, with a maximum load shifting ratio reaching 100% (Davis Energy Group 2007; German et al. 2014). Research conducted by Oak Ridge National Laboratory further revealed that placing insulation on the outer side of structural layers can prolong the load shifting duration of active thermal mass up to 8 h (Jung et al. 2022). Xie et al. (2025) experimentally assessed the load shifting capability of radiant systems with high thermal mass, showing that a 3-h precooling phase could maintain thermal comfort for approximately 2.5 h with minimal energy use. Hu et al. (2020) highlighted that these systems can also leverage the passive thermal mass of the building envelope and reduce peak loads via enhanced radiative heat exchange. This underscores the importance of considering the combined effect of active and passive thermal mass in demand response strategies. In addition to their flexibility benefits, high thermal mass radiant systems have been shown to improve energy efficiency (Kazanci et al. 2016), facilitate renewable energy integration (Carnieletto et al. 2024), and alleviate solar-gain-driven peak cooling loads (Zhao et al. 2022).

Although the flexibility potential of high thermal mass cooling systems is receiving increasing attention, few studies have systematically analyzed how key design parameters such as room geometry, terminal thermal characteristics, and internal heat gains affect both energy flexibility and overall cooling demand. This lack of comparative insight limits the development of effective load shifting strategies. In a study using model predictive control, Hu et al. (2019) observed that shifting cooling operation to off-peak periods could reduce electricity costs but led to increased energy consumption. Ahn et al. (2021) also reported that carpeted radiant floors exhibited a lower peak load reduction (17–29%) compared to bare concrete floors (20–34%). These results underscore the need for more comprehensive analyses to quantify the parameter sensitivities of energy flexibility across varying operating schedules and climatic conditions (Lv et al. 2025).

To address these knowledge gaps, this study conducts an expanded set of parametric simulations beyond what was previously published in a Lv et al. (2025) conference paper to systematically evaluate the energy flexibility characteristics of both floor- and ceiling-based radiant cooling systems. The analysis aims to uncover the fundamental mechanisms through which thermal mass activation modulates cooling loads, thereby establishing a more comprehensive theoretical basis for optimizing the design and operation of high thermal mass radiant systems.

Methodology

The heat exchange process in a radiant air conditioning room is complex, as shown in Figure 1a. The radiant terminal, ventilation system, envelope, fenestration, interior partitions, internal heat sources, and air infiltration all contribute to the transfer or removal of heat within the radiant cooling room. These numerous factors together impact the energy flexibility of the radiant terminals. Additionally, the cold stored within the radiant terminals continues to influence the indoor heat transfer process, making its quantitative justification more complex. In this study, four different typical radiant terminals with high thermal mass (ISO 2012) were considered as shown in Figure 1b, including embedded surface systems (ESS) and thermally activated building systems (TABS) for both floors and ceilings. ESS have an insulating layer that thermally decouples the floor and ceiling surfaces. TABS have the tubing embedded directly in the floor and ceiling structural slab.

Figure 1c presents a workflow to comprehensively investigate the impact of these variables on load shifting performance. The quasi-random sampling method (Sobol 1976) was employed to generate parameter combinations within a multidimensional parameter space. This approach ensures that the parameter combination set accurately captures the true variability of the system. The parameters selected included building window–wall ratio, building orientation, room dimensions (width and length), indoor heat gain levels (jointly by the heat produced from people, lighting, plug loads), the construction of four typical radiant terminals (thermal conductivity and thickness of the slab layer, depth of embedded pipes, and thermal resistance of the cover layer), and operating schedules (determined by start time and duration time, which represent the initiation and continuous period of chilled water supply for the radiant terminals, respectively), resulting in a total of 12,030 distinct case configurations per city. This study presents simulation results for four cities in China and four cities in the United States, along with an additional dataset under fixed start–stop schedules, totaling 108,270 cases.

Then the parameter combinations are used for batch calculations conducted collaboratively with Python and EnergyPlus. In the simulations, the peak and off-peak electricity periods and the typical summer day meteorological conditions were defined according to local utility time-of-use pricing schemes and standard summer day datasets provided by EnergyPlus (China Meteorological Bureau et al. 2005; Wilcox and Marion 2008). For details on the selection of parameter ranges, climate zones and cities, and specific EnergyPlus model settings, refer to the literature (Duarte Roa et al. 2025). The simulation results are collected and analyzed to produce statistical descriptions, and energy flexibility indicators are calculated. Each case preliminarily calculates the appropriate supply water temperature delivered to the radiant terminal, ensuring that the maximum operative temperature during occupancy does not exceed the thermal comfort limit while also accounting for potential

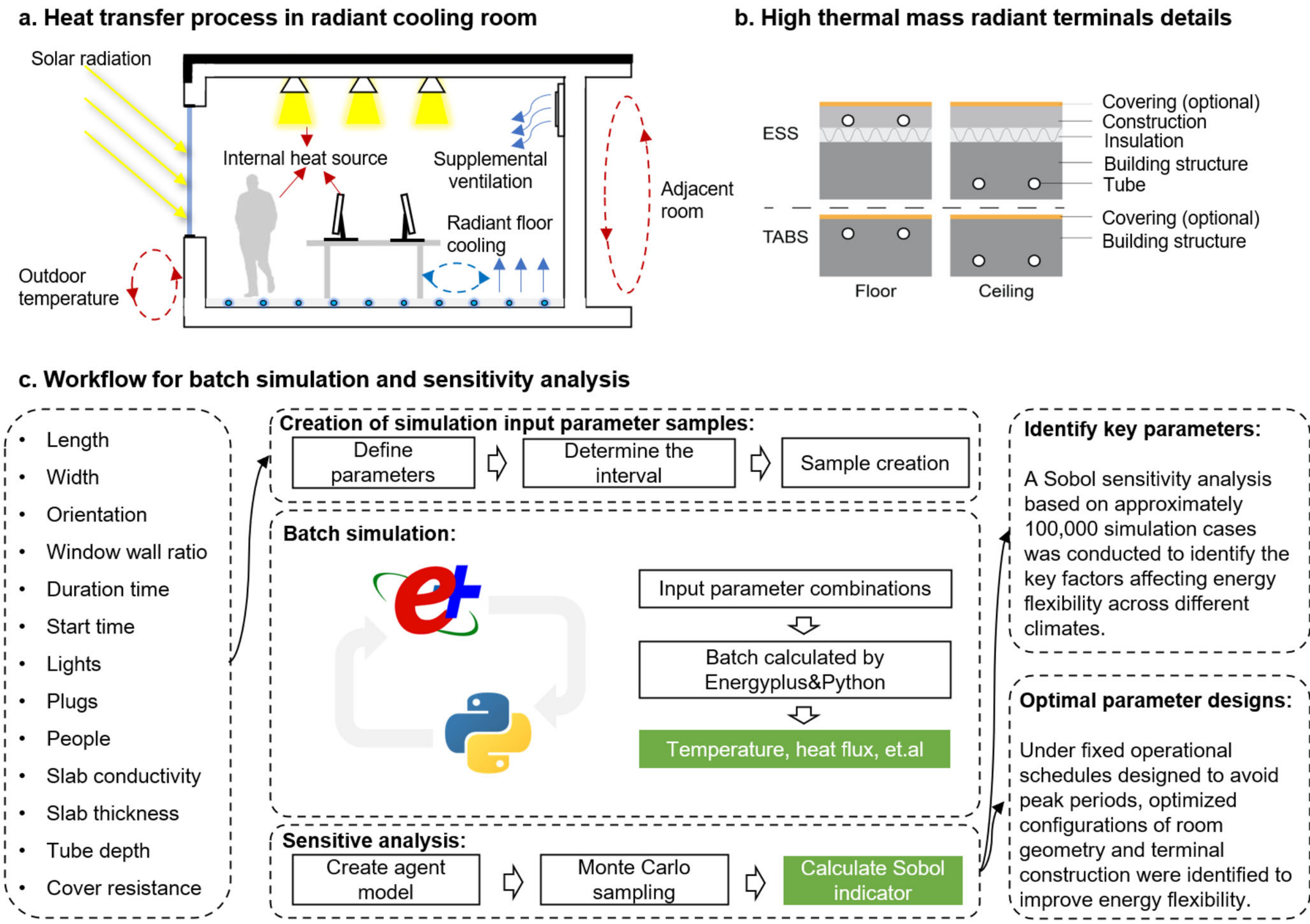

Fig. 1. Schematic of the methodology specification in this study.

condensation risk when the terminal surface temperature approaches the indoor dew point. The supplementary ventilation cooling system is activated synchronously with indoor occupancy and removes the latent load from the indoor environment. Consequently, the model's hourly energy outputs represent the total cooling demand, incorporating both sensible and latent heat components.

Finally, the Sobol sensitivity analysis method (Sobol 1993) is employed for global sensitivity analysis because of its capability to handle nonlinear and multiparameter coupling problems, enabling a comprehensive assessment of the influence of input parameters on the performance of high thermal mass radiant systems (Saltelli et al. 2004). During the calculation of Sobol factors, several agent models were trained using batch simulation results, with the coefficient of determination R^2 greater than 0.96 to ensure the reliability of parameter sensitivity calculations (Sudret 2008; Iooss and Lemaître 2015), and Monte Carlo sampling was employed to enhance the computational efficiency of the calculated Sobol sensitivity indicators (Kucherenko et al. 2009).

The quantitative assessment of building energy flexibility serves as a crucial foundation for the application of auxiliary electricity regulation in buildings. Scholars have proposed indicators and methodological systems to quantitatively evaluate demand flexibility, mainly encompassing aspects of power, energy, and duration. In this study, four performance metrics are employed to evaluate the energy flexibility of concrete-based radiant cooling systems.

The load shifting indicator η_s (Hu et al. 2019) quantifies the relative shift of cooling energy from peak to off-peak periods. A higher value of η_s indicates that a larger share of cooling load is supplied during off-peak hours, reflecting better load shifting performance:

$$\eta_s = \frac{E_{off-peak} - E_{peak}}{E_{off-peak} + E_{peak}} \quad (1)$$

where $E_{off-peak}$ is the cooling energy supplied during the off-peak period, and E_{peak} is the cooling energy supplied during the peak period.

The daily cooling energy density E_A represents the total daily cooling supply of each case, normalized by the floor area of the corresponding room. Used together with η_s, it provides a balanced view of a load shifting strategy's effectiveness, ensuring that improvements in flexibility do not come at the cost of excessive energy use:

$$E_A = \frac{E_{total}}{A} \quad (2)$$

where E_{total} is the total daily cooling energy supplied and A is the conditioned floor area.

The peak cooling load density $P_{\max}$ quantifies the maximum cooling power per unit floor area across individual simulation cases:

$$P_{\max} = \max\left(\frac{P(t)}{A}\right) \tag{3}$$

where $P(t)$ represents the cooling power at time t.

Based on the degree-hour framework (ASHRAE 2020), a new metric is introduced to integrate the accumulated degree-hours during which the indoor operative temperature remains below the thermal comfort threshold, thereby providing an indicator of the cooling level within the room:

$$DH = \sum \left(T_{upper} - T_{op}(t)\right) \cdot \Delta t \tag{4}$$

where T_{upper} is thermal comfort threshold, which in this work was set to 28 °C (GB 50736 2012; ASHRAE 2020), $T_{op}(t)$ is the operative temperature at time t, and Δt is the simulation time step.

The load shifting indicator and cooling supply amount are used together to identify key factors influencing the energy flexibility of high thermal mass radiant systems, while the peak cooling load and accumulated degree-hours are employed as supplementary metrics, as they characterize thermal comfort and cooling power from a time-resolved perspective, making the identification of optimal parameter ranges more robust and practical.

Comparison between Hangzhou and San Francisco

Hangzhou (China) and San Francisco (California, USA) were selected as representative cities because they experience distinct weather patterns, although belonging to similar climate zones—ASHRAE Zone 3 A warm-humid and ASHRAE Zone 3 C marine (International Code Council 2020)—and adopt different time-of-use electricity pricing structures (dual morning–evening peaks versus a single evening peak). In addition, their building envelope constructions differ significantly. These contrasts make them suitable for a comparative analysis in this study.

Load shifting indicator and cooling supply amount

Figure 2 illustrates the operative temperature and cooling load curves from the simulation result datasets for Hangzhou and San Francisco. The gray lines represent all simulation cases, while the colored lines indicate representative cases identified through clustering. Due to differing parameter settings, the results vary across cases. Nevertheless, the operative temperature was maintained below 28 °C in nearly all simulations through preestimation of the supply water temperature, with less than 1% of cases exceeding this threshold and subsequently removed during the data cleaning process.

By integrating the cooling load curves, we derived the daily cooling energy density for each case, hereafter denoted as the cooling supply amount (CSA). Based on the peak and off-peak electricity periods specific to Hangzhou and San Francisco, the load shifting indicator (LSI) was also derived. Figure 3 presents the distributions of LSI and CSA for four types of radiant terminals in the two cities using box-and-whisker plots. Overall, LSI values in Hangzhou are lower than those in San Francisco,

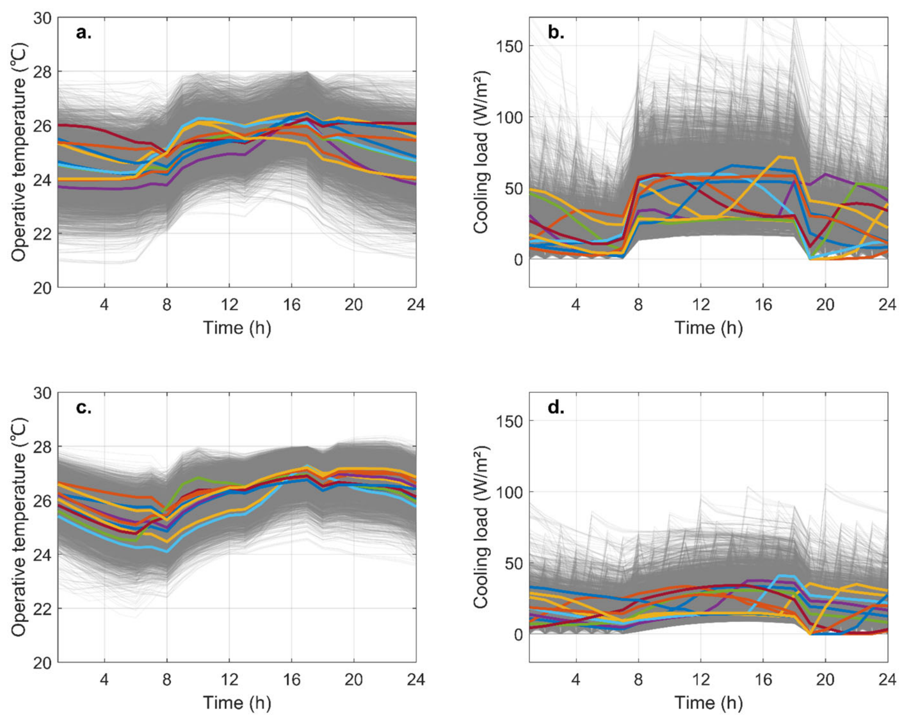

Fig. 2. Statistical results for operative temperature and cooling load curves: (a, b) Hangzhou, (c, d) San Francisco.

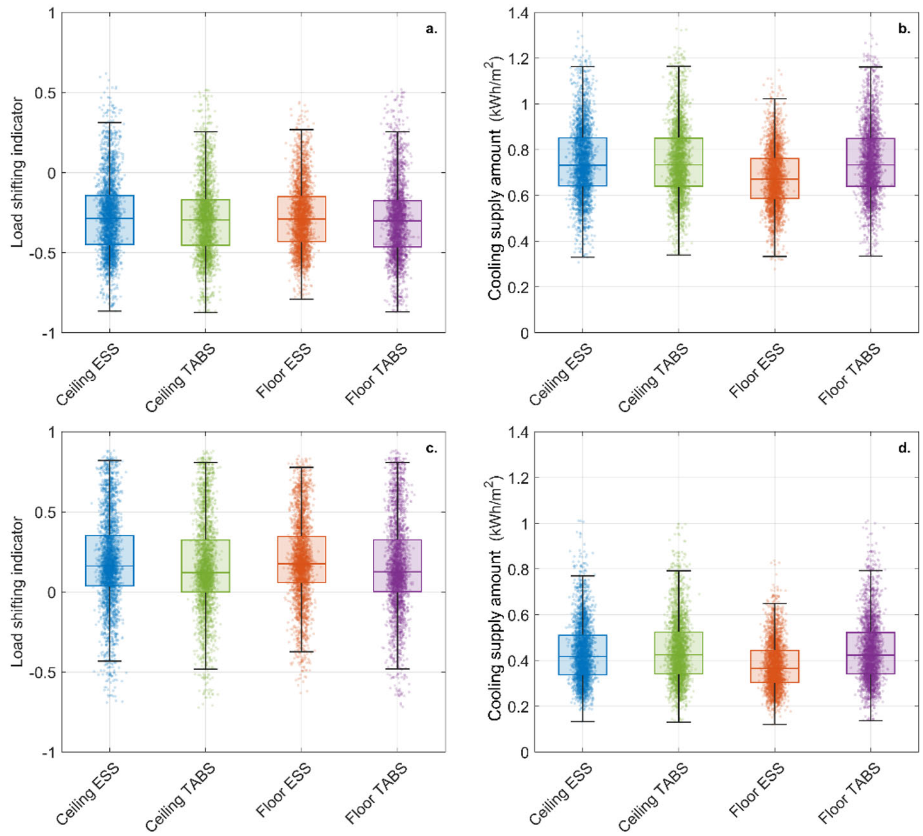

Fig. 3. Statistical results for load shifting and cooling supply amount: (a, b) Hangzhou, (c, d) San Francisco.

primarily due to differences in electricity tariff structures. In San Francisco, the peak period is concentrated between 14:00 and 23:00, whereas in Hangzhou it spans 08:00–11:00 and 13:00–22:00, covering more daytime cooling hours and leaving less time for off-peak load shifting. Additionally, Hangzhou's hotter summer climate results in a significantly higher overall cooling supply amount compared to San Francisco.

Among the four terminal types, the floor ESS (embedded surface system) has a slightly lower cooling supply amount than the others but exhibits the highest median LSI. This performance pattern aligns with its underlying heat-transfer characteristics: Because the insulating layer places the active slab closer to the room side, more of the stored cooling is effectively directed toward the occupied space, resulting in higher load shifting efficiency despite the modest cooling capacity. In contrast, the ceiling ESS demonstrates higher extreme LSI values under certain parameter combinations, indicating greater load shifting potential in specific scenarios, reflecting its stronger load shifting potential in specific scenarios. Its elevated position and distance from major internal heat sources allow it to maintain a lower surface temperature, enabling greater cold accumulation during off-peak periods. For TABS systems, the differences between floor and ceiling configurations are relatively small, as the pipes are embedded directly within the concrete mass; both configurations possess similarly large thermal capacities, and the batch-simulation statistics show no pronounced distinction in their LSI behavior.

Sobol sensitive indicators

Based on the Sobol sensitivity analysis in Figure 4, the key drivers of the LSI are highly consistent across the four high thermal mass radiant terminal types (ceiling ESS, ceiling TABS, floor ESS, and floor TABS) and between the two cities. Among all parameters, start time consistently emerges as the dominant factor with substantially higher Sobol indices than any other variable, followed by duration time as the second most influential parameter in both Hangzhou and San Francisco.

The remaining 11 parameters—including room geometry (length, width, orientation, window-to-wall ratio), internal loads (lighting, plug loads, occupancy density), and radiant terminal construction properties (conductivity, thickness, tube depth, and floor-cover resistance)—exhibit minimal or negligible influence on LSI, though it is noteworthy that in Hangzhou these influences are stronger than in San Francisco, primarily due to the hotter climate conditions. Across all terminal types, only minor differences are observed—for example, TABS systems show slightly lower sensitivity to duration time, likely due to their greater thermal storage capacity, while ceiling systems are marginally more sensitive to envelope-related variables, such as orientation and window-to-wall ratio (WWR). However, these differences are secondary and do not alter the overall conclusion that operation timing dominates.

CSA is an equally important consideration in load shifting strategies. As shown in Figure 4b and d, start time and

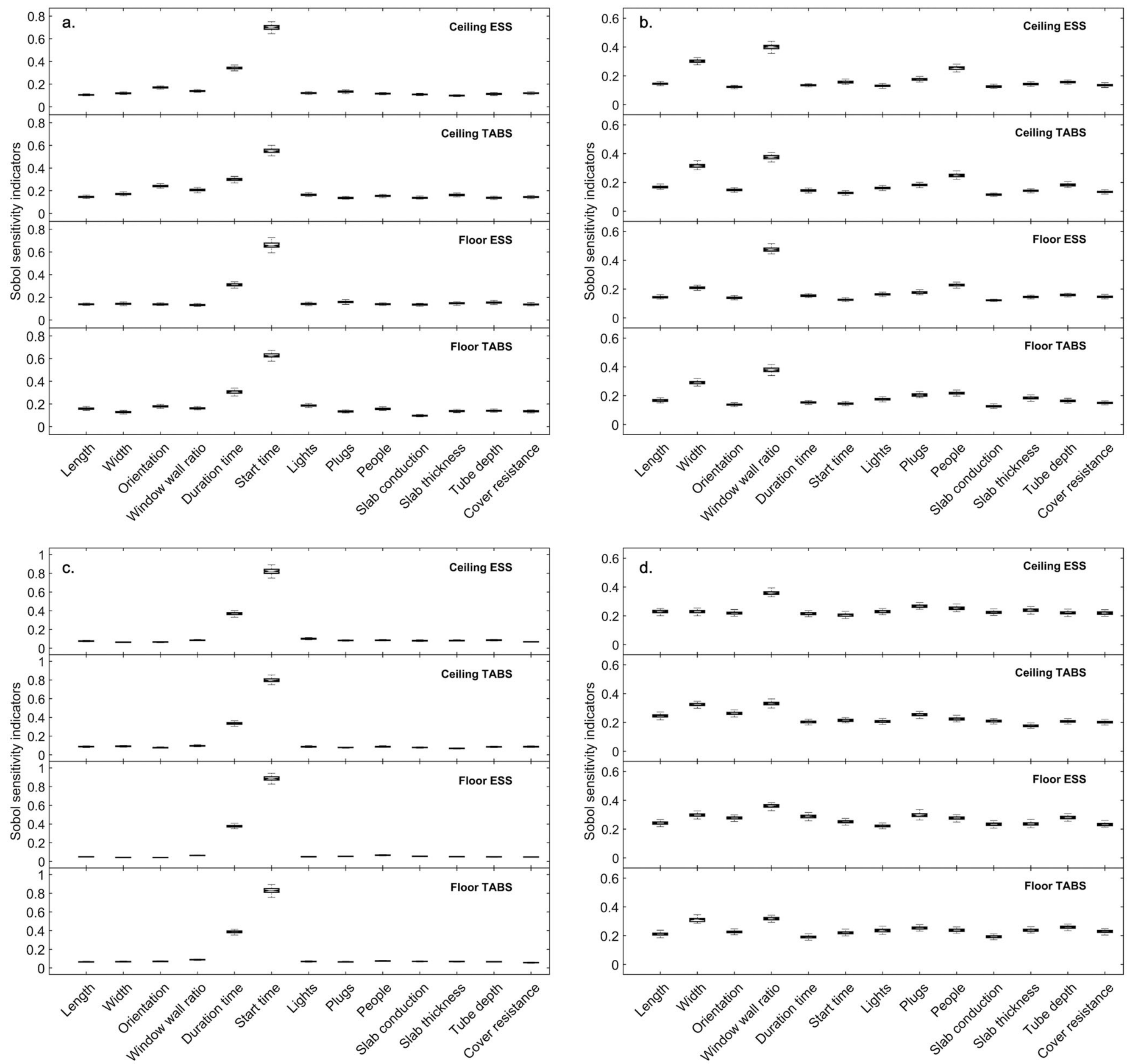

Fig. 4. The results of Sobol sensitivity analysis for the load shifting indicator (LSI) and cooling supply amount (CSA): (a) Hangzhou LSI, (b) Hangzhou CSA, (c) San Francisco LSI, (d) San Francisco CSA.

duration—dominant for LSI—have little to no impact on CSA. Instead, CSA is primarily influenced by room geometry and internal load parameters. At the city level, Hangzhou demonstrates stronger CSA sensitivity to room width compared to San Francisco, reflecting the effects of its hotter summer climate, where a wider room width can help mitigate heat transfer from the building envelope. Notably, the parameter ranking for LSI remains stable across cities despite these climatic differences.

In summary, start time is the most influential parameter for LSI, followed by duration time as the second most important factor, while other variables show relatively weak or negligible effects. Crucially, the dominant LSI parameters are not significant drivers of CSA, suggesting that optimizing start time can substantially improve load shifting performance without materially increasing daily cooling energy use.

Analysis of trends in parameter variations

The Sobol sensitivity results in Figure 4 illustrate the relative importance of each input parameter, showing only minor variation in the ranking across the four high thermal mass radiant terminals. Figures 5 and 6 therefore focus on

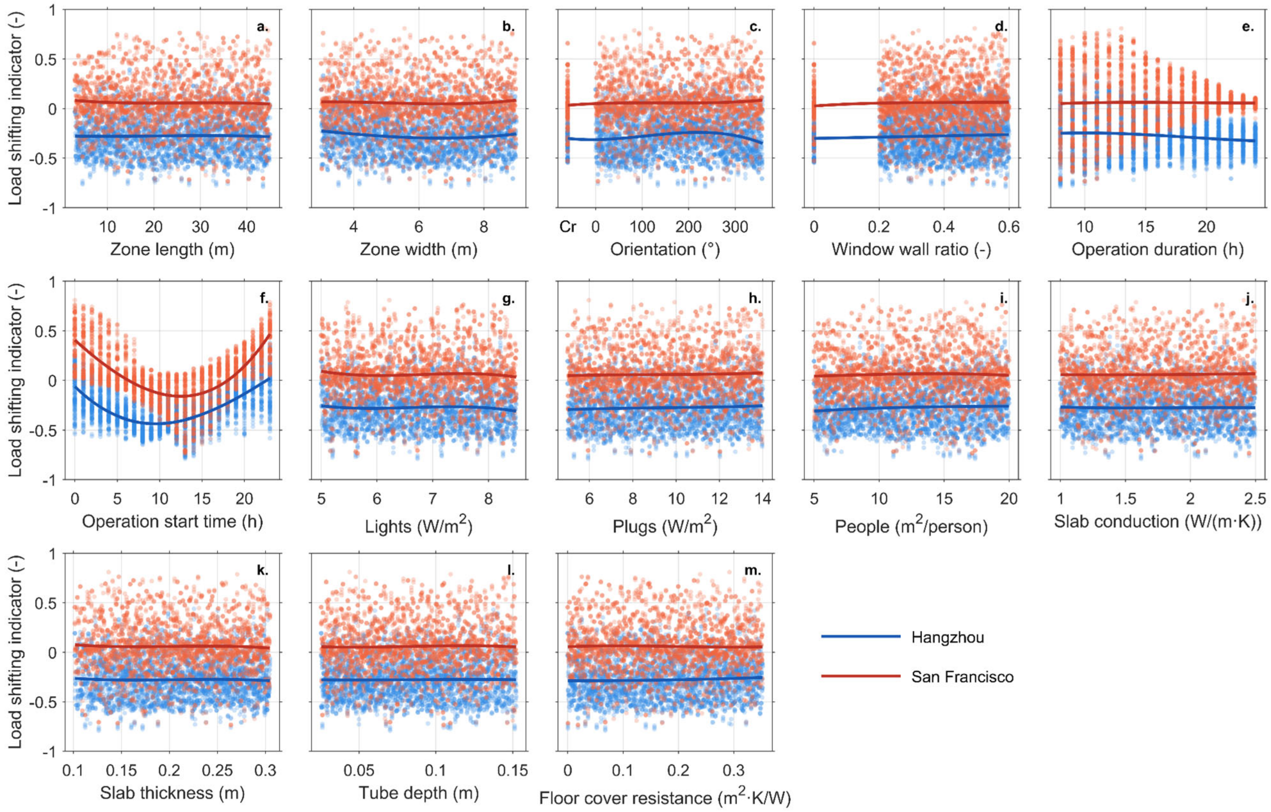

Fig. 5. Relationships between parameters and the load shifting indicator for the floor ESS terminal in Hangzhou and San Francisco.

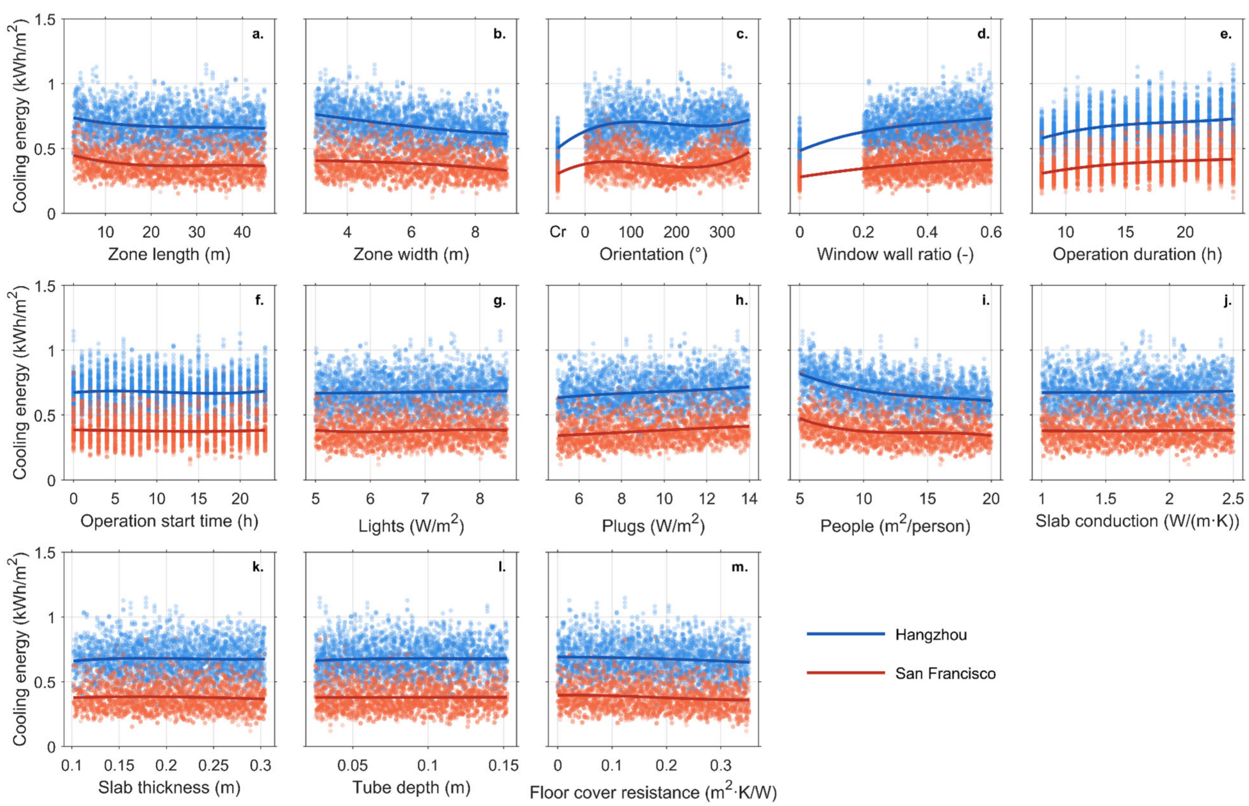

Fig. 6. Relationships between 13 design and operation parameters and the cooling supply amount for the floor ESS terminal in Hangzhou and San Francisco.

the floor ESS terminal as a representative case, providing a detailed visualization of the relationships between 13 input parameters and both the LSI and CSA in Hangzhou and San Francisco. Results for the other terminal types are provided in Appendix A. Overall, CSA values are significantly higher in Hangzhou compared to San Francisco, while LSI values are generally lower. This reflects the increased difficulty of achieving effective load shifting in hotter climates with longer peak pricing periods, where the time window for off-peak operation is more limited due to the combined effects of climate and tariff structure.

For LSI, operation start time is the most influential parameter in both cities, showing a distinct U-shaped relationship: LSI is lowest when operation begins near midday, while early morning or late evening start times substantially enhance load shifting performance. The curvature is steeper in Hangzhou, indicating a stronger marginal impact of scheduling in more constrained conditions. The influence of operation duration varies by city: In Hangzhou, it shows a clear negative correlation with LSI, whereas in San Francisco, it is nearly neutral or slightly positive. This difference is likely due to the broader overlap with peak hours in Hangzhou and the more concentrated peak window in San Francisco. This pattern is consistent with the analysis of variance (ANOVA) results, where operation start time and operation duration both reach strong statistical significance ($p < 0.001$) in the two cities.

Building orientation also exhibits clear city-dependent behavior: In Hangzhou, increasing the orientation angle leads to a significant decrease in LSI ($p < 0.001$), whereas in San Francisco it shows a slight increase ($p = 0.004$). This divergence is likely attributed to differences in solar path and its alignment with peak pricing periods in the two climates. The WWR, internal loads (lights, plug, occupant loads), and the thermal properties of the slab and floor-cover layers—including conductivity, thickness, tube depth, and surface resistance—all show minimal marginal effects on LSI ($p > 0.05$). These findings further indicate that load shifting performance is governed primarily by scheduling decisions rather than by the intrinsic thermal characteristics of the structural components.

For CSA, the trends are generally consistent across both cities. CSA increases with WWR, orientation, operation duration, and internal loads, with stronger responses observed in Hangzhou, likely due to higher cooling demand under hotter conditions. Occupant density shows a significant negative correlation with CSA, as lower density reduces internal heat gains. Zone length and width exhibit a slight negative correlation with CSA, suggesting a limited influence of floor area on unit cooling intensity within the studied range, with the slope of room width being steeper in Hangzhou than in San Francisco. These trends are consistent with the ANOVA results: Room width, orientation, operation duration, WWR, plug loads, and occupant density all show strong statistical significance for CSA in both cities ($p < 0.001$). Similar to the LSI results, the thermal properties of the slab and surface layers—such as thermal conductivity, thickness, tube depth, and surface resistance—exhibit very low sensitivity to CSA, with p values exceeding 0.05 in both cities (e.g., slab conductivity $p = 0.974$ in Hangzhou and $p = 0.544$ in San Francisco; tube depth $p = 0.642$ and 0.294; lighting $p = 0.638$ and 0.218). This indicates that their influence is largely overshadowed by operational and room geometry-related factors.

Start time has a negligible influence on CSA in both locations (Hangzhou: $p = 0.712$; San Francisco: $p = 0.523$), but operation duration shows an upward trend in floor ESS. Specifically, when the operation duration is extended from 8 h to 24 h, a significantly larger increase is observed, reaching 25.9% in Hangzhou and 35.4% in San Francisco. This is largely because for the floor ESS system the relatively small effective thermal mass makes it more prone to overcooling during long operation scenarios, thereby amplifying the increase in CSA. Considering the combined effects with LSI, setting the operation start time at 22:00–23:00 with a duration of 10 h yields favorable LSI performance while keeping CSA nearly unchanged under the tariff structures of both San Francisco and Hangzhou. It is worth noting that for ceiling ESS, ceiling TABS, and floor TABS, the increase is only about 5–9% (6.7–7.6% in Hangzhou, 5.2–8.8% in San Francisco), due to their substantially larger thermal mass. The specific trend of changes can be found in Appendix A.

In summary, the analysis in Figures 5 and 6, together with the sensitivity ranking in Figure 4, suggests that high thermal mass radiant systems can achieve improved load shifting performance primarily by optimizing the operation start time, avoiding peak electricity periods. In addition, operation duration should be carefully controlled to prevent increases in CSA. Within the tested parameter range, substantial improvements in flexibility can be achieved without structural modifications, simply through appropriate scheduling. This provides a clear, practical, and climate-resilient strategy for operational control of high thermal mass radiant systems.

Cross-climate analysis

To investigate the impact of climate variation on the key parameters influencing energy flexibility in high thermal mass systems, four Chinese cities (Hangzhou, Guilin, Nanyang, Chengdu) and four U.S. cities (Miami, Chicago, Seattle, San Francisco) were selected. The cities are arranged along the horizontal axis from cooler to hotter climates. The Chinese cities are all located in the hot summer–cold winter zone, corresponding to ASHRAE Climate Zones 3A/3B, characterized by high summer cooling demand and moderate to high winter heating demand. In contrast, the U.S. cities cover a wider range of ASHRAE climate zones: Miami (Zone 1A, very hot-humid), Chicago (Zone 5A, cool-humid), Seattle (Zone 4C, mixed marine), and San Francisco (Zone 3C, warm marine).

For each city, 12,030 simulations were conducted to calculate the Sobol sensitivity indices of various parameters, followed by a comparative analysis of their magnitudes.

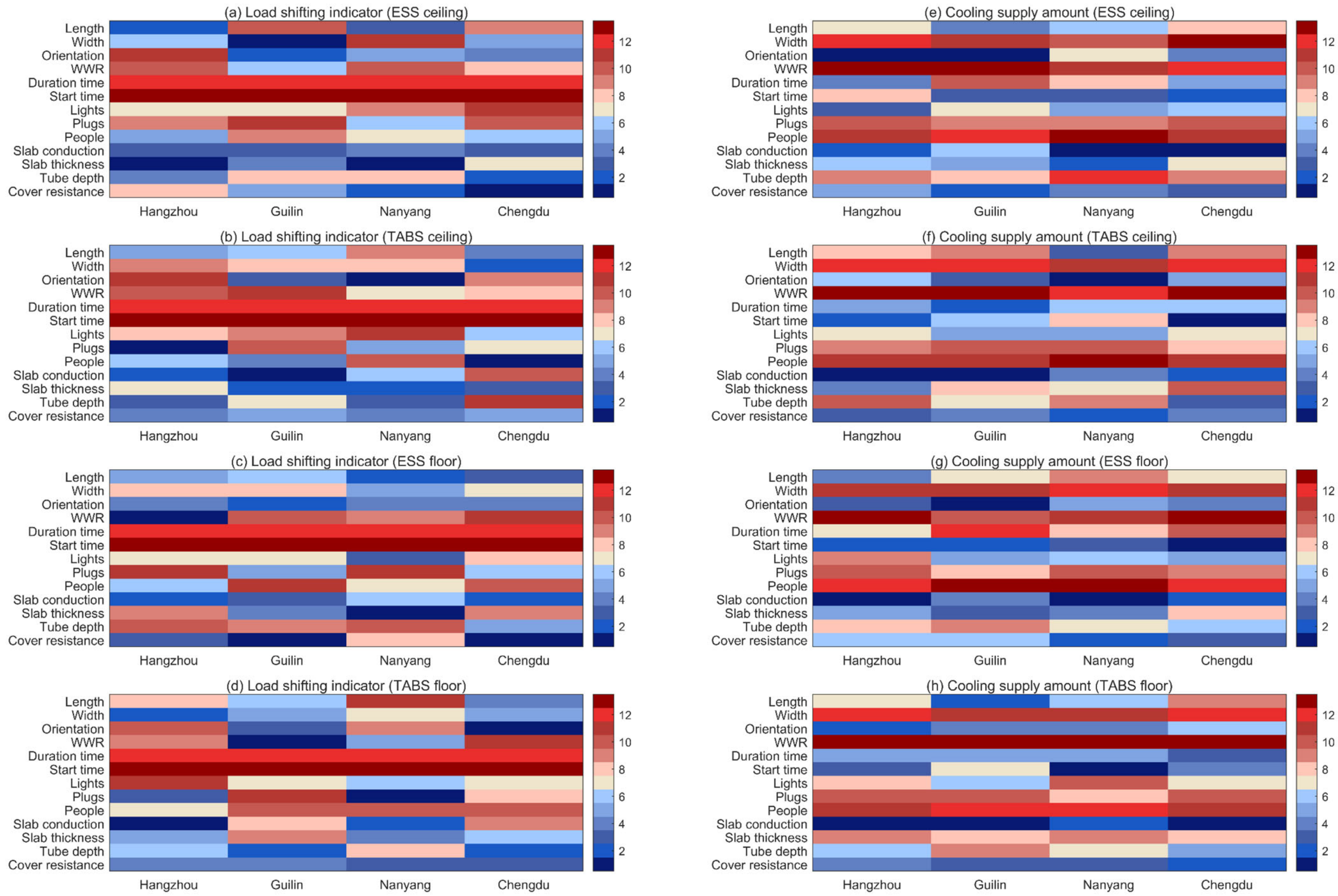

Fig. 7. Parameter importance rankings across four Chinese cities.

Figures 7 and 8 summarize the results, where dark red indicates high importance, and dark blue indicates the lowest importance, that is, the parameter that is least sensitive to LSI or CSA.

For LSI, operation start time consistently ranks first across all climate zones and terminal types, with its importance showing negligible variation with climate conditions. Operation duration is stably ranked second, with similarly small intercity differences. This indicates that regardless of climatic variation, the load shifting capability of high thermal mass radiant systems is primarily driven by operational scheduling. The remaining parameters generally exhibit low importance, with geometric dimensions, occupant density, and slab or floor-cover thermal properties persistently ranking at the bottom. Only in a few scenarios do room geometry parameters (e.g., window-to-wall ratio and orientation) show a slight increase in importance, which is insufficient to alter the overall "start time first and duration second" hierarchy. Differences among terminal types are also small. TABS systems show slightly higher sensitivity to operation duration, while ceiling terminals are marginally more sensitive to room geometry parameters, consistent with their greater thermal storage capacity and exposure to solar gains.

For CSA, the ranking pattern is distinctly different from LSI but remains stable across climate zones. WWR, orientation, and internal loads generally rank among the top factors in most cities and terminal types, whereas operation start time consistently ranks near the bottom, and operation duration shows weak-to-moderate influence. Occupant density exhibits low-to-moderate sensitivity, typically with a negative effect, indicating that lower occupant density reduces internal heat gains and thus cooling demand. Geometric dimensions and slab thermal properties consistently rank at the bottom in nearly all cases.

Despite the wider climatic range in the U.S. cities compared with the Chinese cities, the ranking structure remains highly consistent across climates. LSI is dominated by operation start time and operation duration, while CSA is dominated by room geometry parameters and internal loads. This stability suggests that energy flexibility control strategies for high thermal mass radiant systems have strong applicability and transferability across different climates.

Parametric optimization analysis for enhancing energy flexibility

To further investigate parameter optimization strategies for enhancing energy flexibility in high-thermal-mass radiant cooling rooms, this section fixes the start time and duration at specific values and conducts batch simulations for San Francisco. A sensitivity analysis is then conducted on the

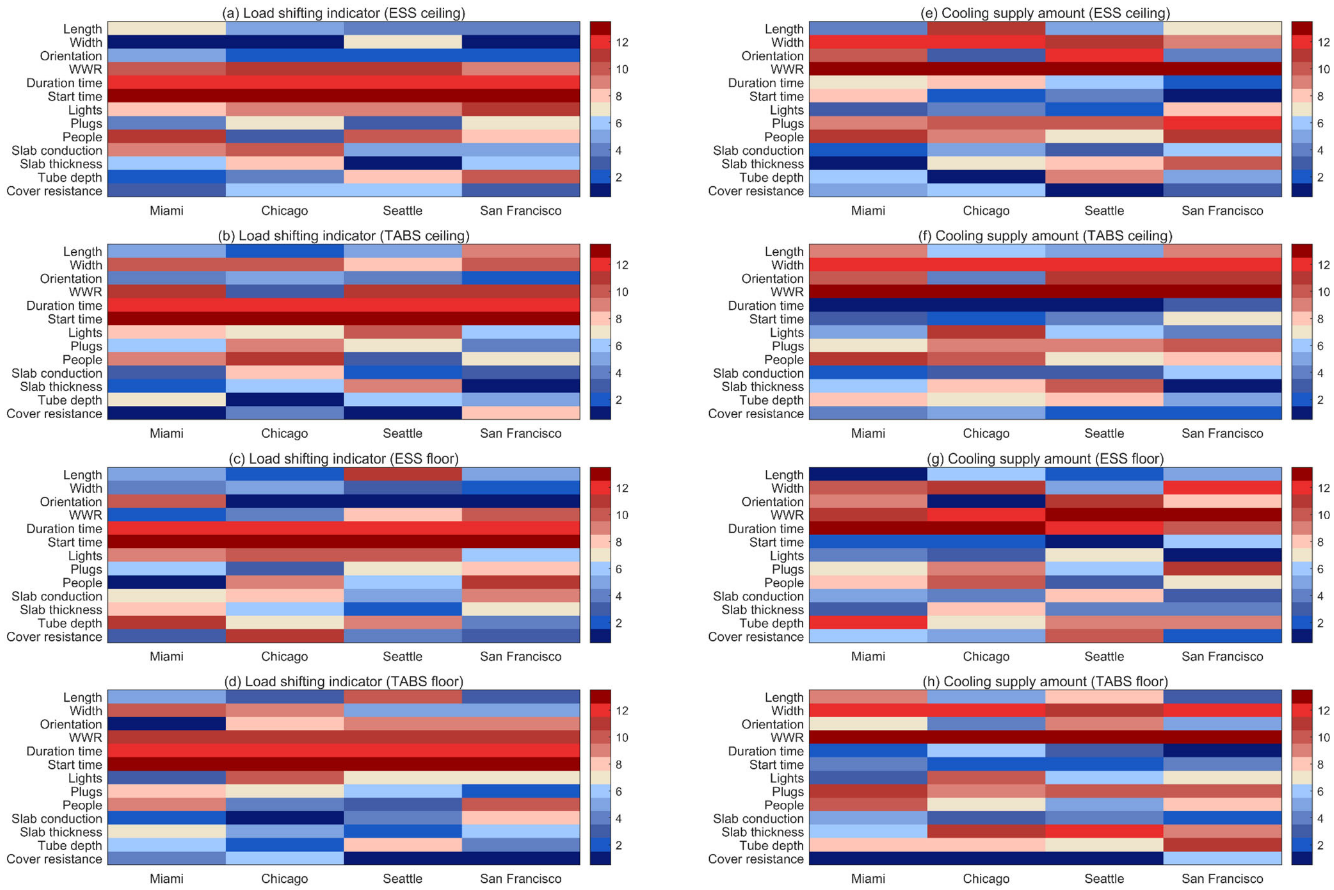

Fig. 8. Parameter importance rankings across four U.S. cities.

resulting dataset, which eliminates the dominant influence of scheduling parameters on load shifting indicator and allows for a clearer examination of the effects of room geometry and radiant terminal design parameters. The fixed operational strategy adopts a start time of 23:00 and a duration of 10 h, a configuration previously shown to promote high load shifting without increasing cooling supply amount in the preceding analysis. In addition to the previously analyzed load shifting indicator and cooling supply amount, this analysis also considers comfort performance degree-hours and peak cooling load (Figure 9c and d) to provide a more comprehensive evaluation of energy flexibility performance for parameter optimization.

Under flexible scheduling, LSI was almost entirely dominated by the start time and duration time parameters. In contrast, under the fixed schedule scenario (Figure 9a), where both start time and duration are constrained, second-tier design parameters emerged as the dominant drivers. Specifically, window-to-wall ratio (WWR), orientation, lighting, and plug loads showed significantly higher sensitivity across all terminal types. This suggests that in the absence of scheduling flexibility, these parameters govern the temporal distribution of cooling energy, thereby determining the load shifting potential. In addition, thermophysical design variables—including slab thermal conductivity, thickness, embedded tube depth, and cover resistance—exhibited moderate sensitivity, with ceiling TABS systems showing slightly stronger responses. This is because the ceiling slab's large thermal mass is largely insulated from direct solar and internal heat gains, causing its thermal behavior to depend primarily on structural heat conduction and therefore on the terminal's design parameters.

The sensitivity structure for CSA remained highly consistent between the flexible and fixed scheduling scenarios (Figure 9b). In both cases, WWR was the most influential factor, followed by other heat gain-related parameters such as orientation, lighting, and plug loads. Thermophysical properties of radiant terminals consistently showed very low sensitivity in both datasets, indicating that daily cooling demand is primarily driven by solar exposure and internal heat gains rather than by thermal mass effects. In Figure 9c, orientation emerged as the most influential parameter, with room width also showing relatively high sensitivity. Unlike the other performance metrics, DH displayed generally higher sensitivity across a wider range of variables, suggesting that adjustments to room geometry, internal heat sources, and radiant terminal design can all effectively influence comfort outcomes. In the peak cooling load analysis shown in Figure 9d, the window-to-wall ratio (WWR) generally stands out as the most influential parameter across most radiant terminal types. However, in the ceiling ESS system, building orientation surpasses WWR in sensitivity, becoming the dominant factor. This distinct pattern arises because WWR primarily affects the magnitude of window-related

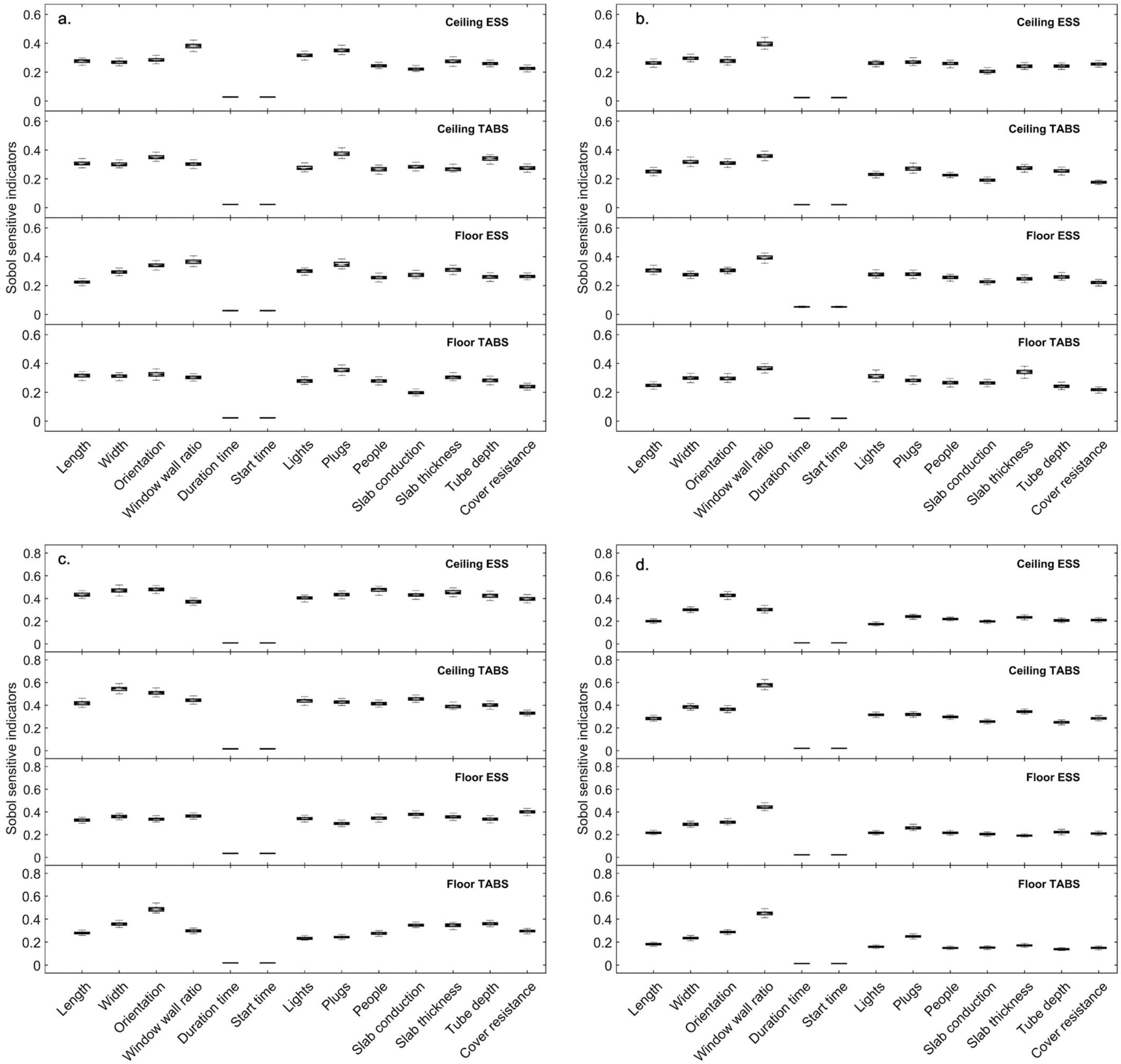

Fig. 9. Sobol sensitivity indicators under fixed operational schedule: (a) load shifting indicator, (b) cooling supply amount, (c) cooling degree-hours below 28 °C, (d) peak cooling load.

solar gains, whereas orientation determines the timing of peak solar heat gains. Since the ceiling ESS surface does not directly receive solar radiation and has relatively small thermal mass, its peak cooling load becomes more strongly governed by the timing of façade heat gains, making orientation more influential than WWR for this terminal type. In addition, building width also exhibits relatively high sensitivity in all cases.

Figure 10 presents a comparative analysis of LSI and CSA under a fixed nighttime precooling strategy (starting at 23:00 and lasting for 10 h) versus the flexible scheduling dataset. Under flexible scheduling, LSI varies between approximately −0.44 and 0.81, while under fixed scheduling, it increases to 0.41–0.89. CSA remains nearly the same under both scheduling strategies, as shown in Figure 10b. These results indicate that in temperate climates such as San Francisco, a fixed nighttime precooling strategy is generally more advantageous, as it can achieve higher LSI without increasing the CSA.

As shown in Figure 11, for LSI under fixed scheduling, several envelope and geometric parameters exhibit noticeably different influences compared with the dataset in which the start time and duration were varied. In particular, the window-to-wall ratio (WWR) shows a clear positive correlation with LSI: Cases with WWR = 0.20 ± 0.05 yield an average load shift of approximately 0.70, whereas those with

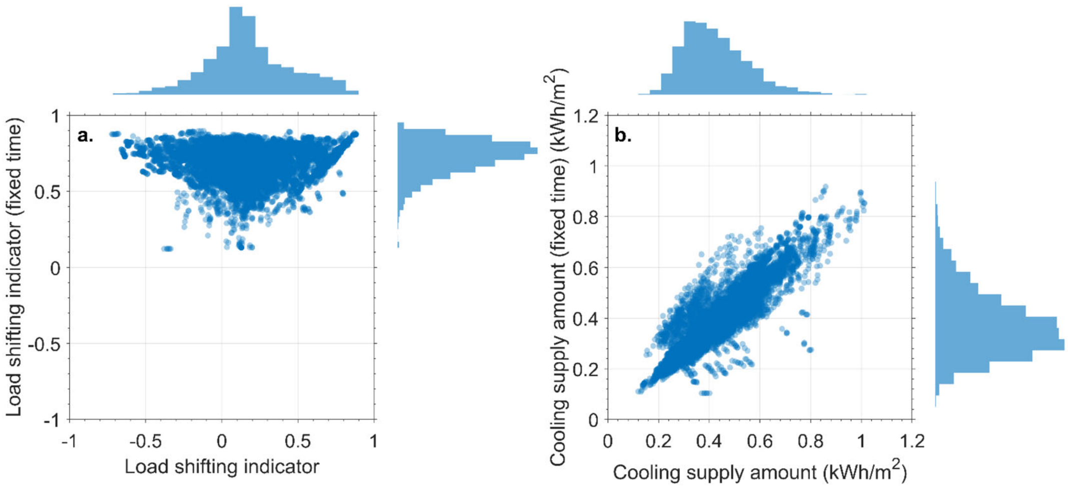

Fig. 10. Scatter histogram of load shifting indicator and cooling supply amount.

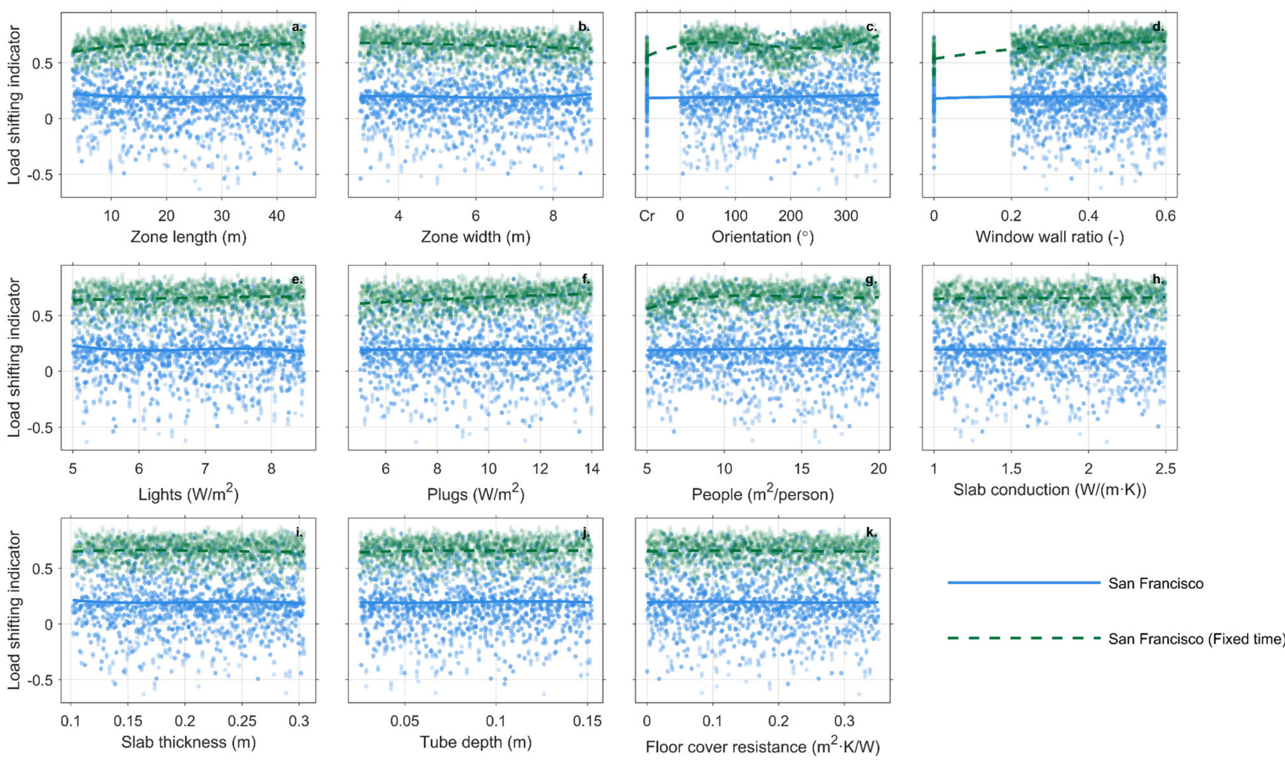

Fig. 11. Variation in load shifting indicator with parameters under fixed vs. flexible scheduling for floor ESS.

WWR $= 0.60 \pm 0.05$ increase to 0.78, indicating a substantial enhancement in load shifting performance as façade openness increases. In contrast, within the variable-time dataset, this variation is much smaller. Zone length also demonstrates a positive relationship and zone width shows a negative correlation. Building orientation exhibits a bimodal sensitivity pattern with peaks in the east and west facing directions. These trends are closely related to the role of these parameters in heat gain.

As illustrated in Figure 12, the parameter sensitivities for CSA are largely consistent between fixed and flexible schedules. WWR, orientation, lighting, and plug loads show clear positive correlations with CSA, reinforcing the understanding that daily cooling demand is primarily governed by solar and internal heat gains. Occupancy density presents a negative correlation with CSA, indicating that lower internal gains reduce energy demand. The terminal construction parameters have little influence on CSA under both scenarios, indicating that they primarily affect the cooling transfer process rather than the total cooling demand.

Figure 13 illustrates the parameter sensitivities for degree-hours below 28 °C (DH). A larger DH indicates a

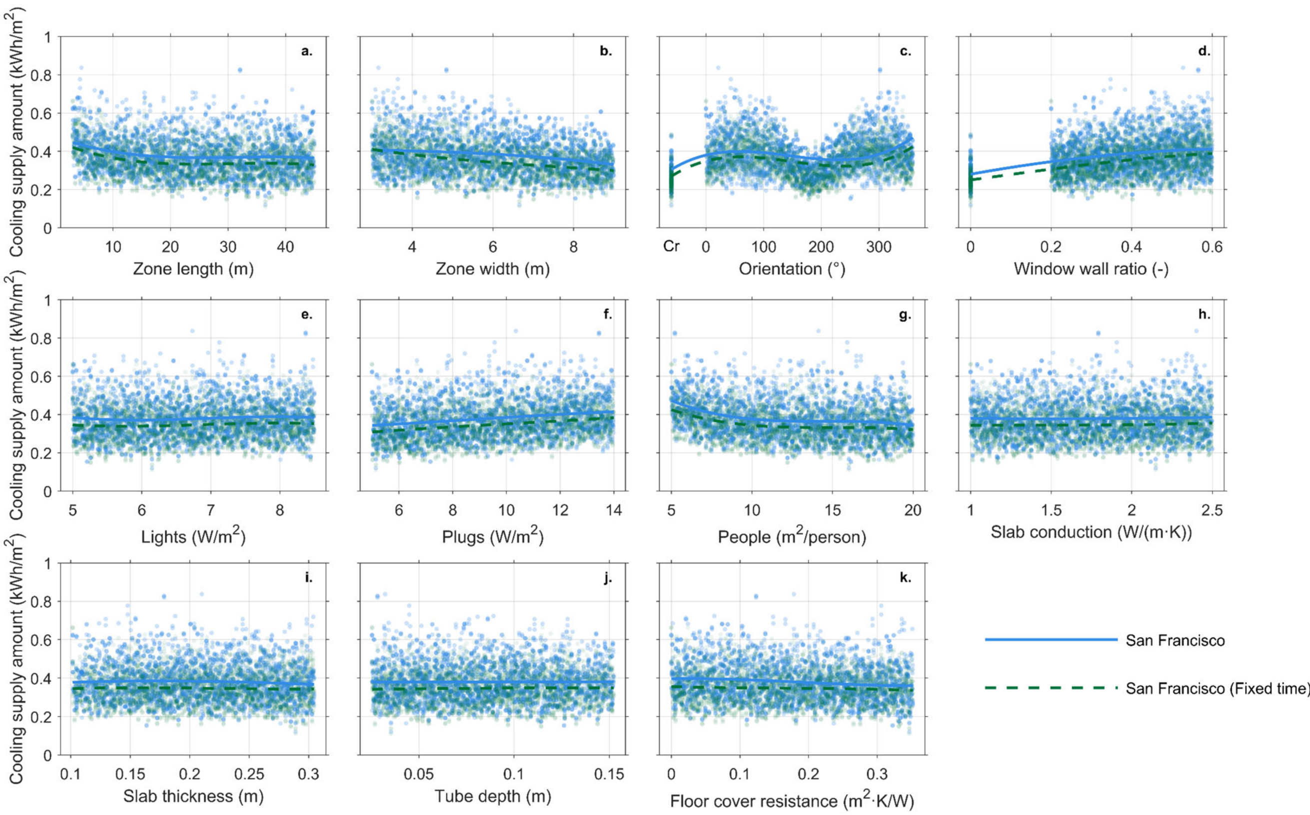

Fig. 12. Variation in cooling supply amount with parameters under fixed vs. flexible scheduling for floor ESS.

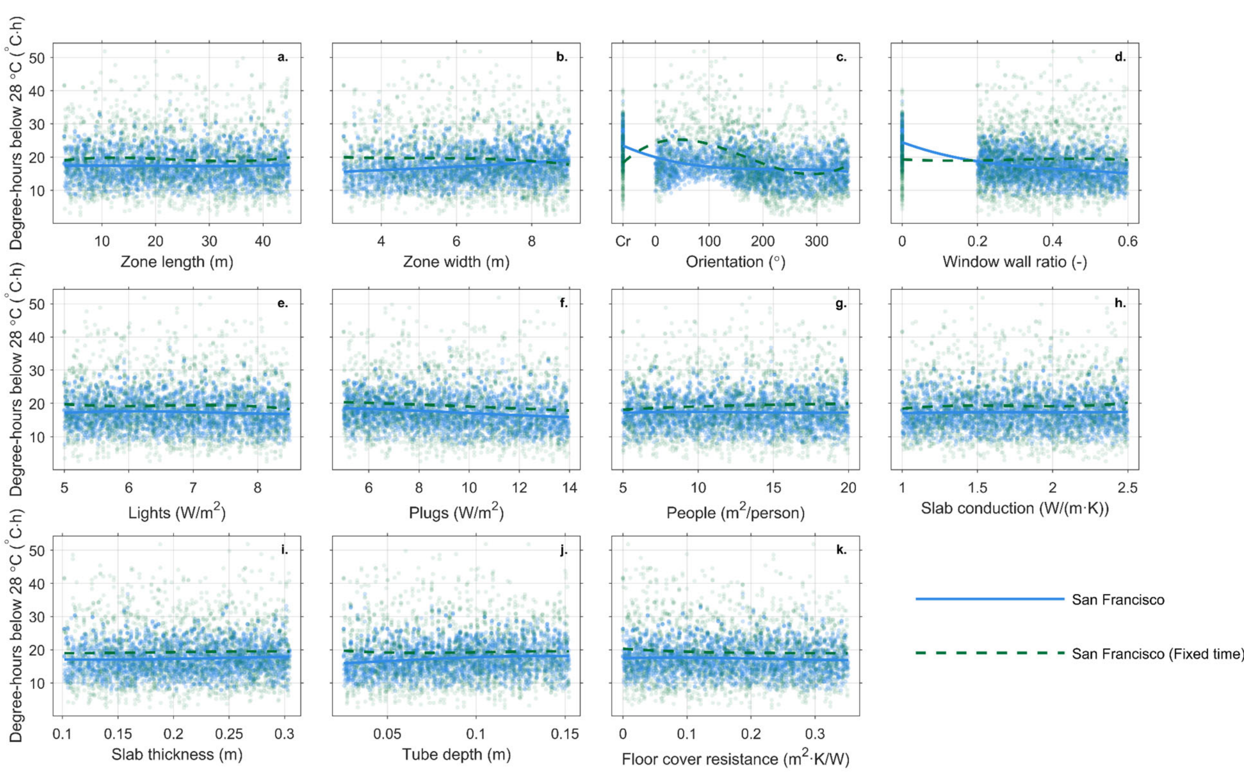

Fig. 13. Variation in degree-hours below 28 °C with parameters under fixed vs. flexible scheduling for floor ESS.

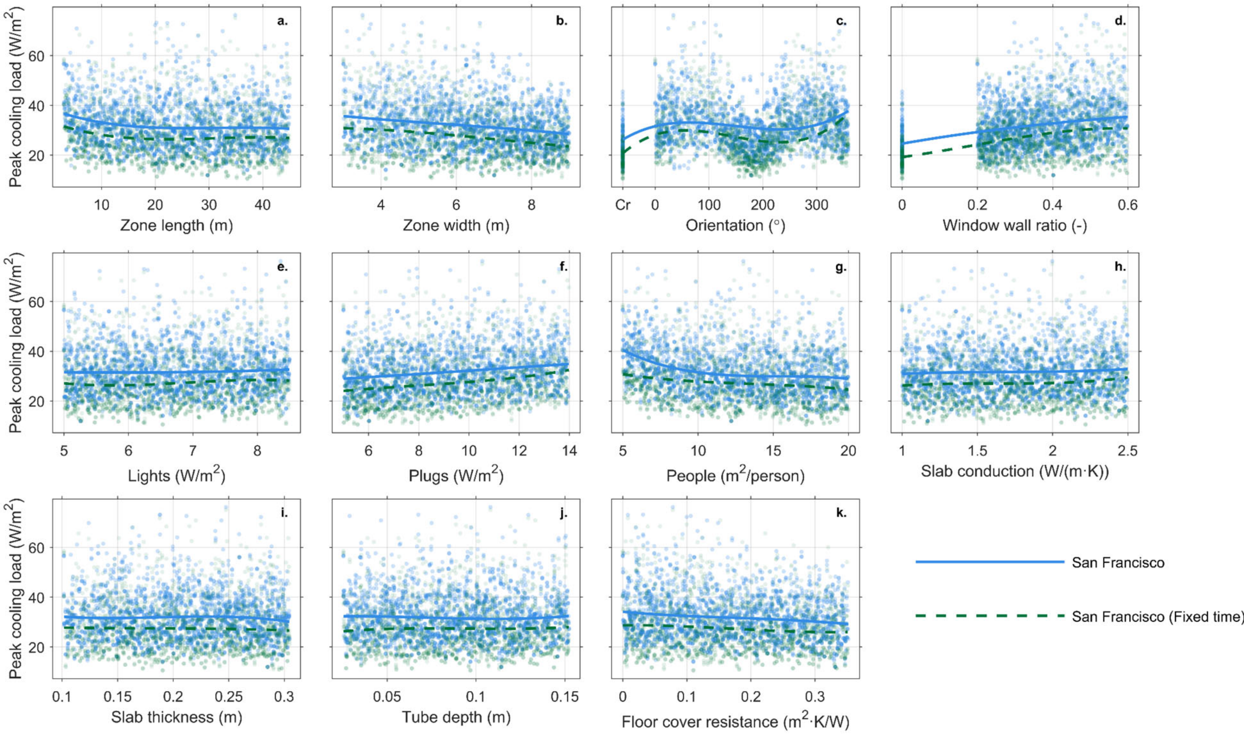

Fig. 14. Variation in peak cooling load with parameters under fixed vs. flexible scheduling for floor ESS.

greater margin by which the indoor temperature remains below the 28 °C threshold, thus reflecting better comfort resilience. Orientation emerges as the most sensitive parameter for DH. Compared with the dataset that allows varying operation times, the fixed-time scenario benefits from sufficient nighttime precooling, resulting in significantly higher DH values for east-facing rooms (orientation 90°). However, west-facing rooms (orientation 270°) experience a substantial decrease in DH, highlighting their vulnerability to afternoon solar exposure. This suggests that under deep precooling strategies, optimization for west-facing rooms is particularly critical and should be given greater design attention.

Figure 14 illustrates the parameter relationships for peak cooling load (PCL). Under fixed operating schedules, the room undergoes deep nighttime precooling, and the cooling supplied by the radiant terminal on the water side is temporally offset from the supplemental ventilation cooling. As a result, PCL remains consistently lower compared with the flexible scheduling scenario. For the floor ESS system, the average PCL across all sample cases is 2.06 W/m^2 (6.51%) lower, clearly demonstrating the benefits of controlled scheduling. Since in the fixed-time dataset the radiant terminal ceases chilled water circulation after 9:00, the sensitivity to orientation becomes more pronounced. In terms of sensitivity distribution, PCL closely resembles that of CSA, with window-to-wall ratio, orientation, lighting, and occupancy density remaining the primary drivers. However, unlike CSA, floor cover resistance shows a much stronger negative correlation with PCL, underscoring its role in peak load suppression.

From the preceding analysis, it can be observed that to enhance energy flexibility in high thermal mass systems, several key design strategies emerge from the parametric evaluation. A primary consideration is the control of solar exposure and internal heat gains. Reducing the WWR, within reasonable limits for daylighting and visual comfort, proves to be an effective lever. Orientations that receive intense solar radiation—especially western exposures—should be avoided or mitigated through external shading devices or spectrally selective glazing. At the same time, minimizing internal loads from lighting and plug equipment can substantially reduce both CSA and PCL, while also improving thermal comfort as measured by degree-hours below 28 °C. Importantly, under sufficient nighttime precooling, the sensitivity of the thermophysical design parameters of radiant terminals is further suppressed, particularly for the degree-hour and peak cooling load metrics, which indicates that operational strategies and room geometry choices can often be more decisive than detailed material properties in determining overall system flexibility.

Discussion

This study clarifies a long-standing unresolved question in high thermal mass radiant cooling: the question of which system parameters primarily determine energy flexibility. Analysis across multiple cities, climates, and four radiant terminal types shows that start/stop timing is the dominant driver of load shifting indicator (LSI), with operation duration as a secondary factor. By contrast, cooling supply amount (CSA) is governed mainly by room geometry and internal heat gains rather than start or duration time. This decoupling is encouraging, as it indicates that designers and operators can substantially enhance flexibility through optimized scheduling without increasing daily energy use, provided that envelope and internal loads remain within reasonable limits.

The cross-climate analysis reinforces the transferability of these findings. Even though absolute cooling demand and tariff peak periods differ among cities, the hierarchy of drivers remains stable. As the heat level rises across cities, the importance of operation duration rises, while start time consistently remains the dominant parameter. This trend can be explained by the fact that, with higher thermal severity, the proportion of heat gain transmitted through the building envelope becomes a larger fraction of the total building heat gain, thereby reducing the overall variance caused by fluctuations in internal heat sources. Consequently, in high heat level regions, the statistical range of load shifting under different parameter combinations converges more rapidly as the operation duration increases, while CSA is dominated by window-to-wall ratio (WWR). This supports a two-stage optimization pathway: (1) adjust operational schedules to avoid tariff peaks, and (2) refine design parameters to reduce solar and internal loads, thereby controlling CSA and peak cooling demand. Subtle differences exist across terminal types—for example, the floor ESS shows slightly higher sensitivity to operation duration, possibly due to its relatively lower thermal mass content compared with other types of radiant terminals (see Figure 1b).

The fixed nighttime deep-precooling scenario is particularly instructive. When scheduling freedom is removed (fixed start at 23:00, 10-h duration), second-tier parameters—especially WWR, orientation, lighting, and plug loads—emerge as the main determinants of LSI. In other words, once operation is already aligned to avoid peak tariffs, room geometry and internal load control become the key levers for enhancing flexibility.

Naturally, this study has limitations. The analysis is based on typical-day weather and tariff representations and relies on a limited set of indicators to characterize cooling demand. Although the Sobol method captures global sensitivities, results may vary under extreme façades, dynamic tariffs, or mixed-mode operation. In addition, the study adopts schedule-based rather than predictive control; with weather and occupancy forecasting, further gains are likely. These caveats do not undermine the core conclusions but instead highlight opportunities for implementation refinements.

Ultimately, the creation of cooling energy flexibility depends on how cooling storage and release are managed under surplus or shortage conditions. Building heat gains determine the cooling energy required to maintain comfort during occupancy, while the operating strategy and structural configuration of radiant terminals govern storage and discharge. In this study, the minimum single operation duration exceeds 8 h, under which radiant systems generally reach steady state. As a result, the thermophysical design of the radiant terminals shows limited influence on flexibility metrics—a trend especially evident under fixed nighttime deep-precooling conditions.

Conclusion

This cross-climate, large-scale parametric analysis provides clear design-stage guidance for grid-interactive high thermal mass radiant cooling systems. Results show that operation start time is the primary driver of load shifting indicator across all climates and terminal types, followed by operation duration, enabling significant flexibility gains without increasing the cooling supply amount. In contrast, cooling supply amount is mainly influenced by window-to-wall (WWR) ratio, orientation, and internal loads, highlighting the importance of controlling building heat gains and internal heat sources. These driver hierarchies remain consistent across different climates and terminal types—from floor to ceiling systems—demonstrating strong applicability. Furthermore, under parametric simulations with fixed start and duration times, the analysis reveals the optimization of design parameters for enhancing energy flexibility performance, with low WWR and favorable orientation being particularly critical. Both parameters highlight the role of controlling solar gains, indicating that mitigating solar radiation is essential for improving system flexibility. Overall, the findings support a two-stage optimization pathway: first, optimize operational schedules to maximize load shifting potential; second, refine room geometry and radiant terminal parameters to maintain comfort and reduce peak cooling loads without increasing energy use.

Disclosure statement

No potential conflict of interest was reported by the authors.

Funding

This work was supported by Zhejiang Provincial Key R&D Program of China (No. 2023C03152), and the Center for the Built Environment at the University of California, Berkeley.

ORCID

Carlos Duarte Roa http://orcid.org/0000-0002-5129-2969
Kang Zhao http://orcid.org/0000-0003-1721-9423

References

Ahn H et al. 2021. How can floor covering influence buildings' demand flexibility? Energies (Basel). 14(12):3658. https://doi.org/10.3390/en14123658

ASHRAE. 2020. ANSI/ASHRAE Standard 55-2020: thermal environmental conditions for human occupancy. American Society of Heating, Refrigerating and Air-Conditioning Engineers.

Braun JE. 1990. Reducing energy costs and peak electrical demand through optimal control of building thermal storage. ASHRAE Trans. 96(2):876–887.

Carnieletto L, Kazanci OB, Olesen BW, Zarrella A, Pasut W. 2024. Combining energy generation and radiant systems: challenges and possibilities for plus energy buildings. Energy Build. 325:114965. https://doi.org/10.1016/j.enbuild.2024.114965

China Energy News. 2023 Jun 29. Zhejiang electric power enhances flexible load control capacity for air conditioners.

China Meteorological Bureau, C. I. Center, C. D. Office, and Tsinghua University, Department of Building Science and Technology. 2005. China standard weather data for analyzing building thermal conditions. China Building Industry Publishing House.

Davis Energy Group. 2007. SMUD off-peak over-cooling project: final report. California Energy Commission, PIER—Renewable Energy Technologies Division.

Duarte Roa C, Raftery P, Schiavon S, Bauman F. 2025. How high can You Go: determining the warmest supply water temperature for high thermal mass radiant cooling systems under thermal comfort constraints. Energy Build. 331:115387.

Gallardo A, Berardi U. 2022. Evaluation of the energy flexibility potential of radiant ceiling panels with thermal energy storage. Energy. 254:124447. https://doi.org/10.1016/j.energy.2022.124447

GB 50736. 2012. GB 50736-2012 design code for heating, ventilation and air conditioning of civil buildings. China Architecture & Building Press.

German A, Hoeschele M, Springer D. 2014. Maximising the benefits of residential pre-cooling. In: Proceedings of the ACEEE Summer Study on Energy Efficiency in Buildings. Pacific Grove, CA.

Heptonstall PJ, Gross RJK. 2020. A systematic review of the costs and impacts of integrating variable renewables into power grids. Nat Energy. 6(1):72–83. https://doi.org/10.1038/s41560-020-00695-4

Hu M, Xiao F, Jørgensen JB, Li R. 2019. Price-responsive model predictive control of floor heating systems for demand response using building thermal mass. Appl Therm Eng. 153:316–329. https://doi.org/10.1016/j.applthermaleng.2019.02.107

Hu R, Liu G, Niu J. 2020. The impacts of a building's thermal mass on the cooling load of a radiant system under various typical climates. Energies (Basel). 13(6):1356. https://doi.org/10.3390/en13061356

Huang S, Katipamula S, Lutes R. 2021. Experimental investigation on thermal inertia characterization of commercial buildings for demand response. Energy Build. 252:111384. https://doi.org/10.1016/j.enbuild.2021.111384

IEA. 2023. Space cooling. International Energy Agency.

International Code Council. 2020. International Energy Conservation Code (IECC) 2021. International Code Council.

Iooss B, Lemaître P. 2015. A review on global sensitivity analysis methods. In: Dellino G, Meloni C, editors. Uncertainty management in simulation-optimization of complex systems: algorithms and applications. Springer US. p. 101–122. https://doi.org/10.1007/978-1-4899-7547-8_5

ISO. 2012. Building environment design—design, dimensioning, installation and control of embedded radiant heating and cooling systems. International Organization for Standardization.

Jung S et al. 2022. Peak cooling load shift capability of a thermal energy storage system integrated with an active insulation system in US climate zones. Energy Build. 277:112484. https://doi.org/10.1016/j.enbuild.2022.112484

Kazanci OB, Shukuya M, Olesen BW. 2016. Theoretical analysis of the performance of different cooling strategies with the concept of cool exergy. Build Environ. 100:102–113. https://doi.org/10.1016/j.buildenv.2016.02.013

Kucherenko S, Rodriguez-Fernandez M, Pantelides C, Shah N. 2009. Monte Carlo evaluation of derivative-based global sensitivity measures. Reliab Eng Syst Saf. 94(7):1135–1148. https://doi.org/10.1016/j.ress.2008.05.006

Lv G, Duarte Roa C, Zhao K, Ge J. 2025. Energy flexibility and sensitivity analysis of high thermal mass radiant terminals. Presented at the ASHRAE Winter Conference Proceedings, 2025, Orlando, FL. https://doi.org/10.63044/w25dua98

Lv G, Zhao Z, Zhao K, Ge J. 2024. The building decarbonization in high-density cities: challenges and solutions. ASME J Eng Sustain Build Cities. 5(4):040801 (12 pp). https://doi.org/10.1115/1.4066503

Neukomm M, Nubbe V, Fares R. 2019. Grid-interactive efficient buildings technical report series: overview of research challenges and gaps (No. NREL/TP-5500-75470, DOE/GO-102019-5227, 1577966) (p. NREL/TP-5500-75470, DOE/GO-102019-5227, 1577966). Washington, DC: U.S. Department of Energy. https://docs.nlr.gov/docs/fy20osti/75470.pdf

O'Shaughnessy E, Shah M, Parra D, Ardani K. 2022. The demand-side resource opportunity for deep grid decarbonization. Joule. 6(5): 972–983.

Olesen B. 2008. Radiant floor cooling systems. ASHRAE J. 50(9):16–22.

Olsthoorn D, Haghighat F, Moreau A, Lacroix G. 2017. Abilities and limitations of thermal mass activation for thermal comfort, peak shifting and shaving: a review. Build Environ. 118:113–127. https://doi.org/10.1016/j.buildenv.2017.03.029

Saltelli A, Tarantola S, Campolongo F, Ratto M. 2004. Sensitivity analysis in practice: a guide to assessing scientific models. John Wiley & Sons.

Sobol IM. 1976. Uniformly distributed sequences with an additional uniform property. USSR Comput Math Math Phys. 16(5):236–242. https://doi.org/10.1016/0041-5553(76)90154-3

Sobol IM. 1993. Sensitivity estimates for nonlinear mathematical models. Math Modell Comput Exp. 1:407.

Sudret B. 2008. Global sensitivity analysis using polynomial chaos expansions. Reliab Eng Syst Saf. 93(7):964–979. https://doi.org/10.1016/j.ress.2007.04.002

Tang H, Wang S, Li H. 2021. Flexibility categorization, sources, capabilities and technologies for energy-flexible and grid-responsive buildings: state-of-the-art and future perspective. Energy. 219:119598. https://doi.org/10.1016/j.energy.2020.119598

Vivian J, Chiodarelli U, Emmi G, Zarrella A. 2020. A sensitivity analysis on the heating and cooling energy flexibility of residential buildings. Sustain Cities Soc. 52:101815. https://doi.org/10.1016/j.scs.2019.101815

Wilcox S, Marion W. 2008. User's manual for TMY3 data sets. No. NREL/TP-581-43156. National Renewable Energy Laboratory.

Xie Y, Li Y, Cui H. 2025. Experimental investigation and scenario-based optimization of energy flexibility in embedded radiant cooling systems. Case Stud Therm Eng. 67:105835. https://doi.org/10.1016/j.csite.2025.105835

Xu R, Liu X, Liu X, Zhang T. 2024. Quantifying the energy flexibility potential of a centralized air-conditioning system: a field test study of hub airports. Energy. 298:131313. https://doi.org/10.1016/j.energy.2024.131313

Zhao K, Lv G, Shen C, Ge J. 2022. Investigating the effect of solar heat gain on intermittent operation characteristics of radiant cooling floor. Energy Build. 255:111628. https://doi.org/10.1016/j.enbuild.2021.111628

Appendix A. Variation of load shifting indicator and cooling supply amount with parameters

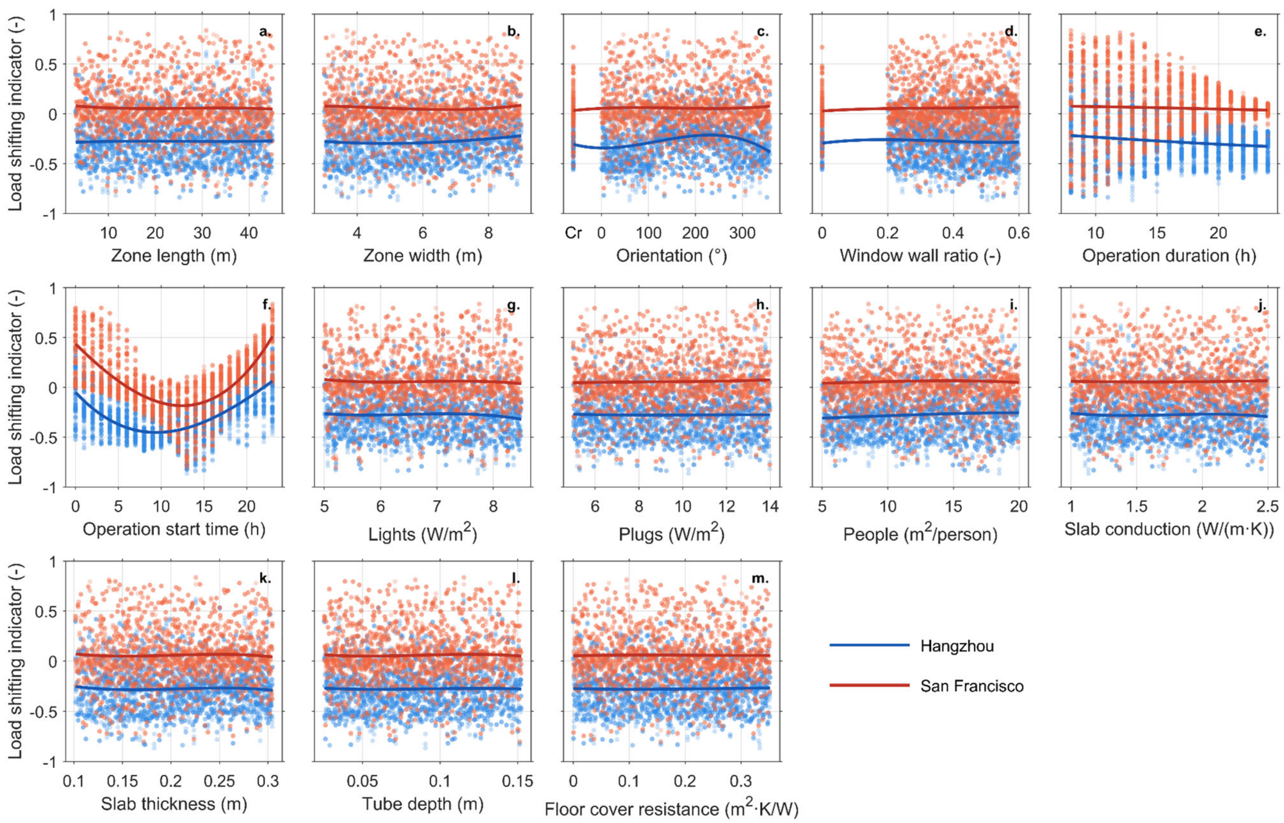

Fig. A1. Relationships between parameters and the load shifting indicator for the ceiling ESS terminal in Hangzhou and San Francisco.

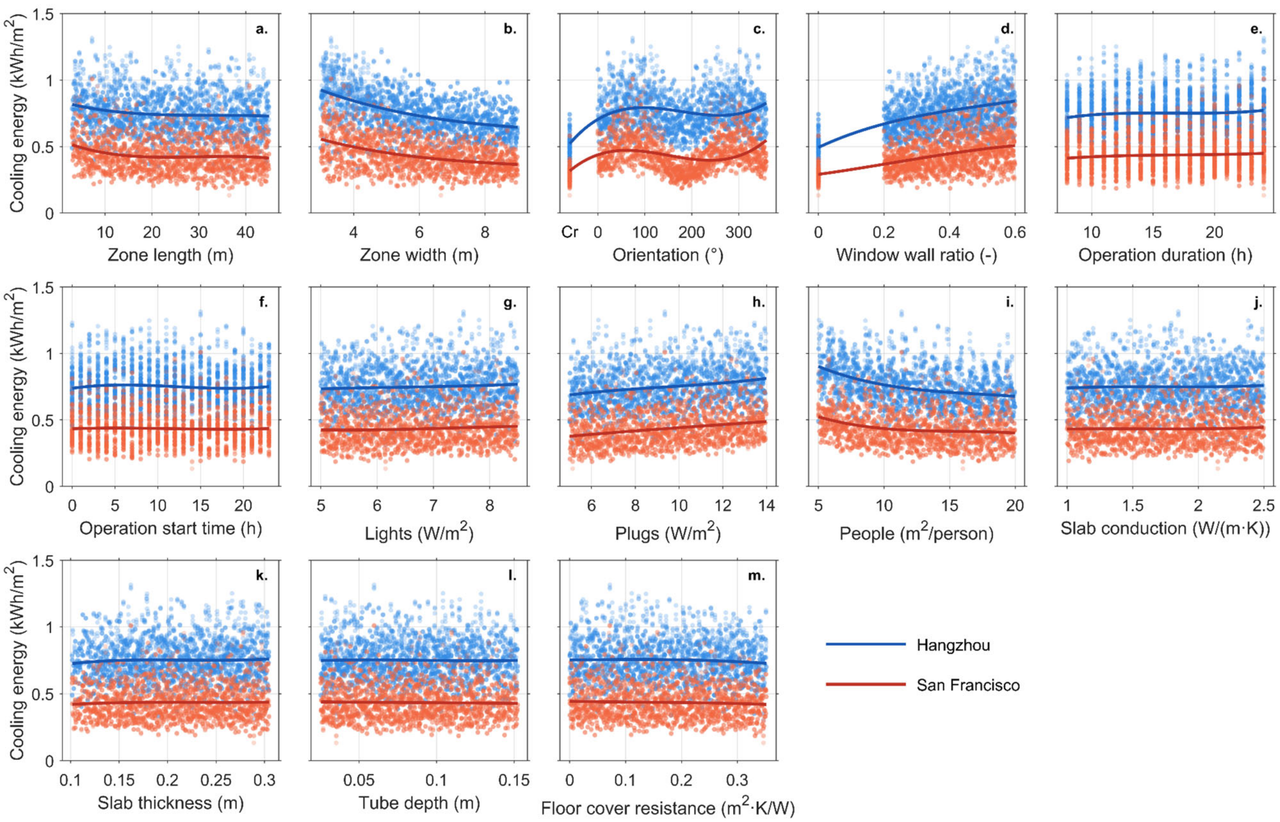

Fig. A2. Relationships between parameters and the cooling supply amount for the ceiling ESS terminal in Hangzhou and San Francisco.

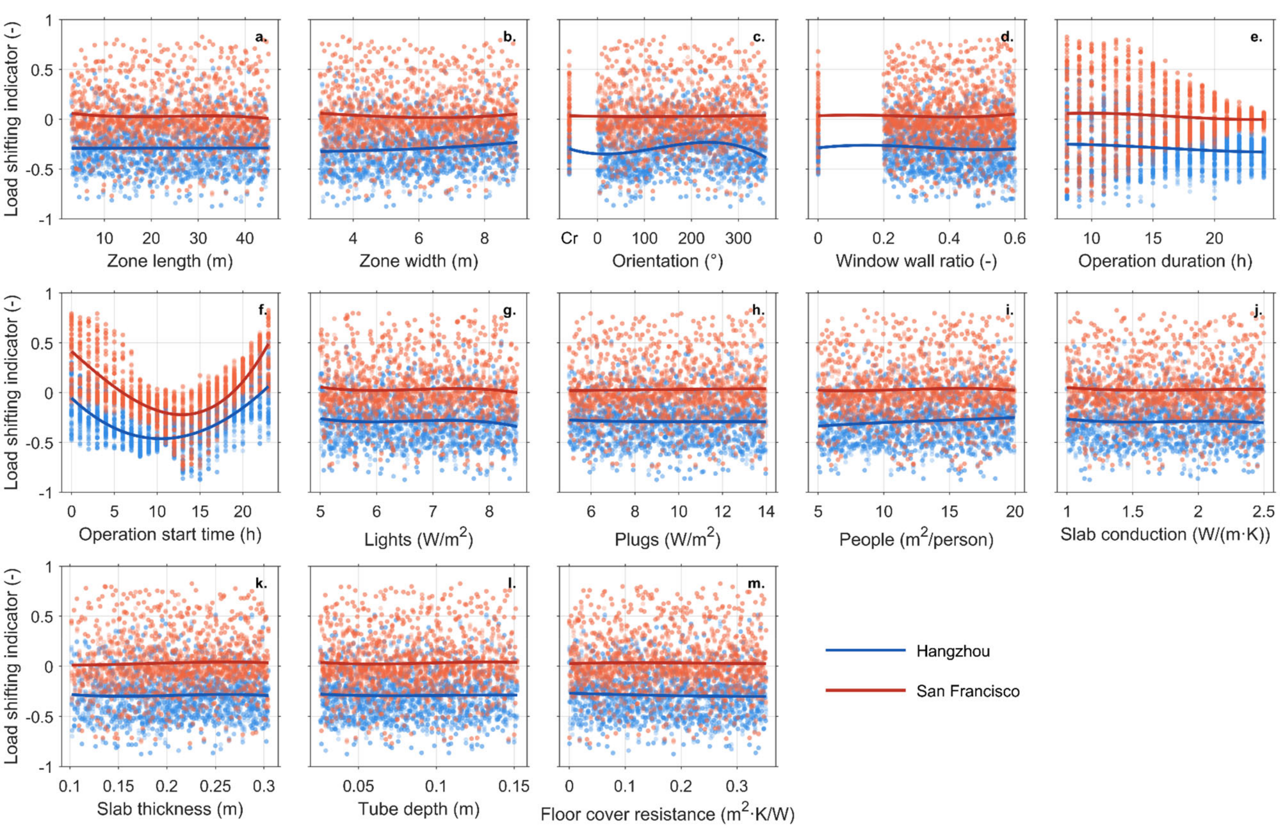

Fig. A3. Relationships between parameters and the load shifting indicator for the ceiling TABS terminal in Hangzhou and San Francisco.

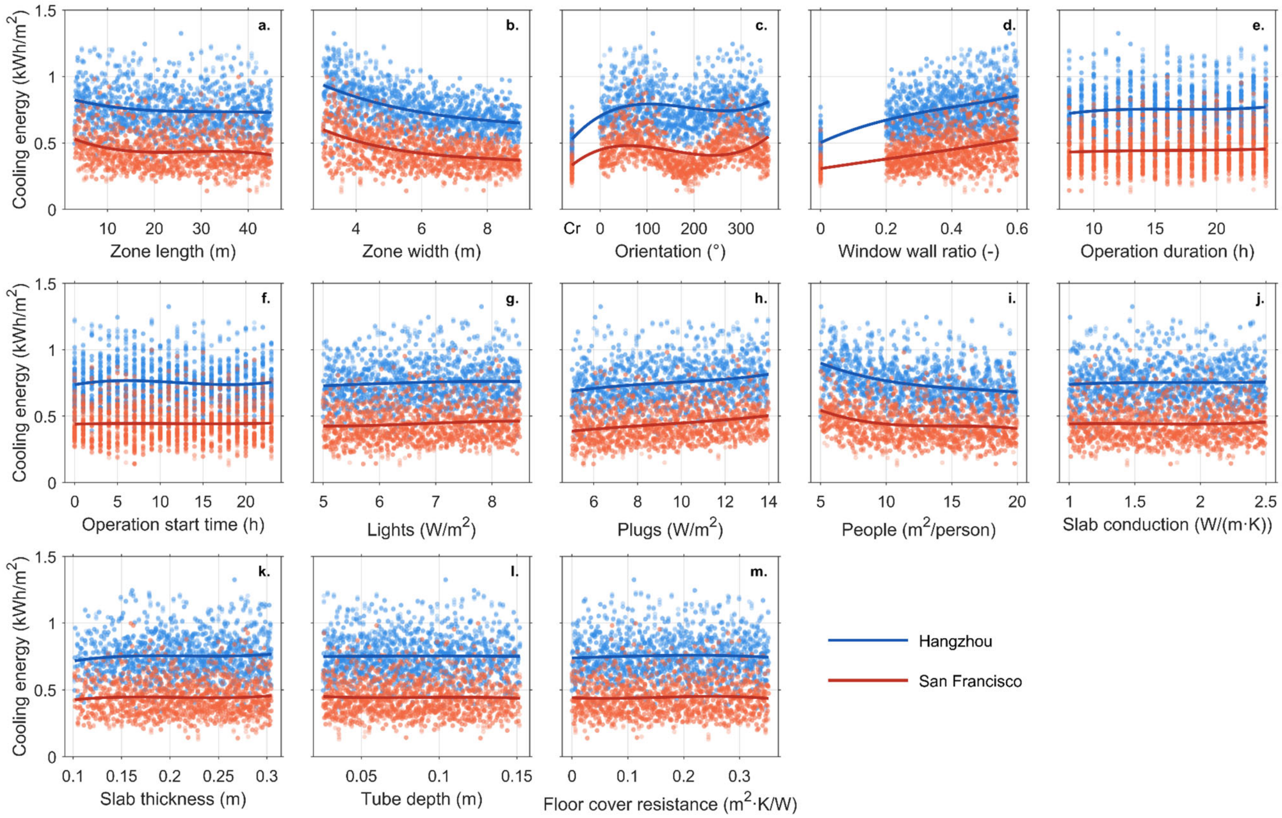

Fig. A4. Relationships between parameters and the cooling supply amount for the ceiling TABS terminal in Hangzhou and San Francisco.

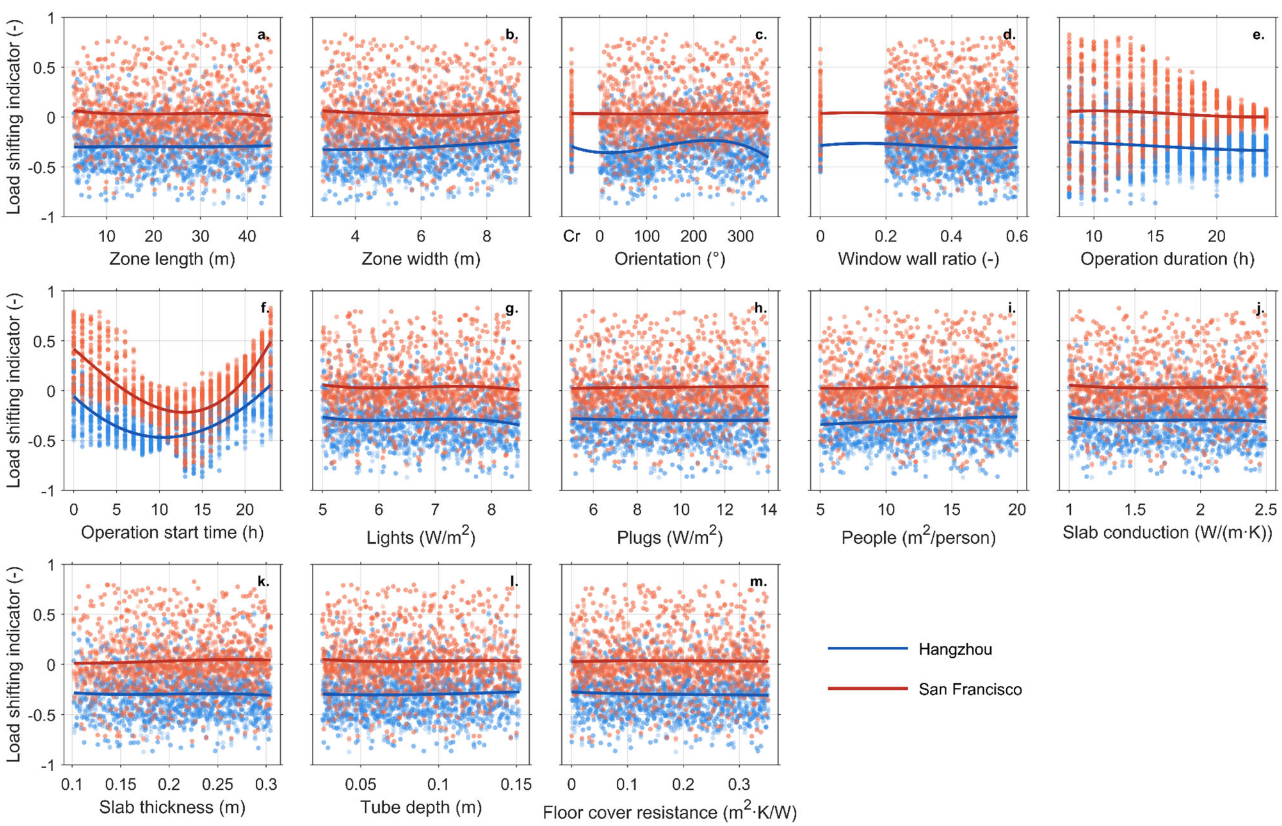

Fig. A5. Relationships between parameters and the load shifting indicator for the floor TABS terminal in Hangzhou and San Francisco.

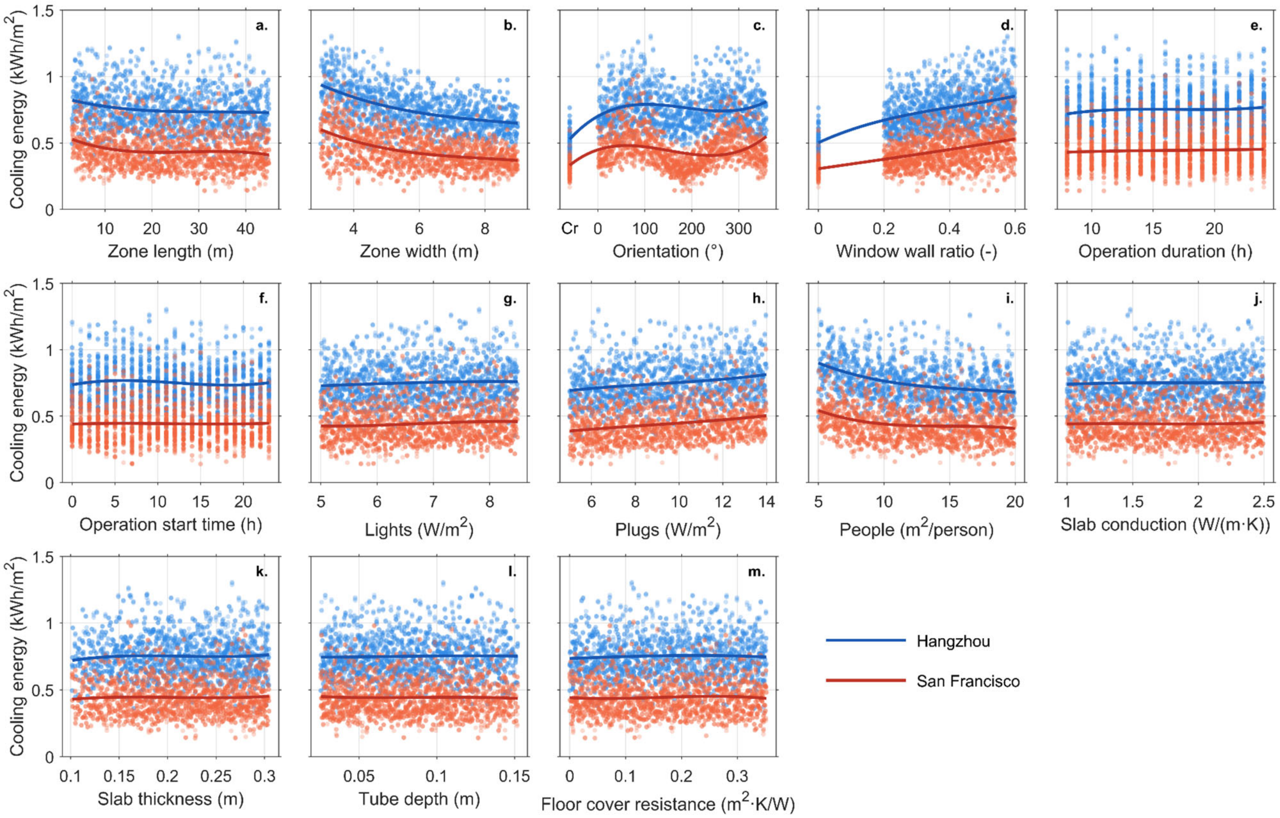

Fig. A6. Relationships between parameters and the cooling supply amount for the floor TABS terminal in Hangzhou and San Francisco.

Appendix B. Parameter variation trends of fixed scheduling

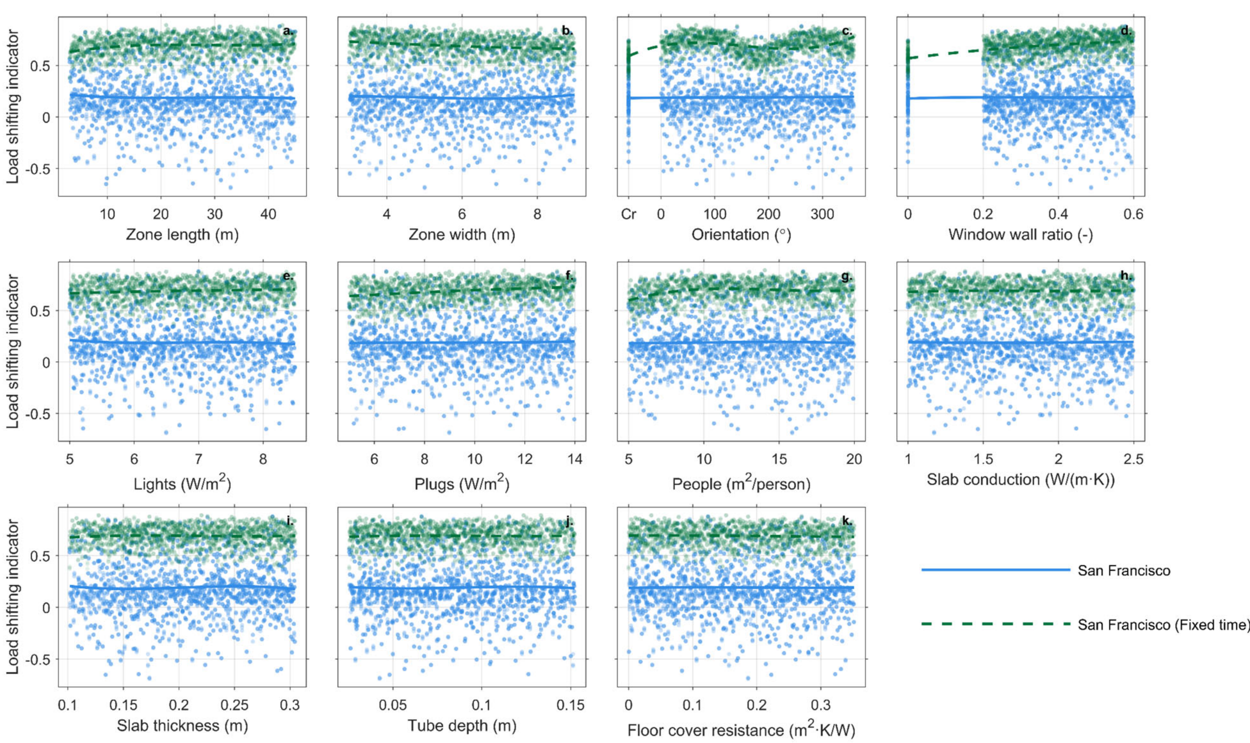

Fig. B1. Variation in load shifting indicator with parameters under fixed vs. flexible scheduling for ceiling ESS.

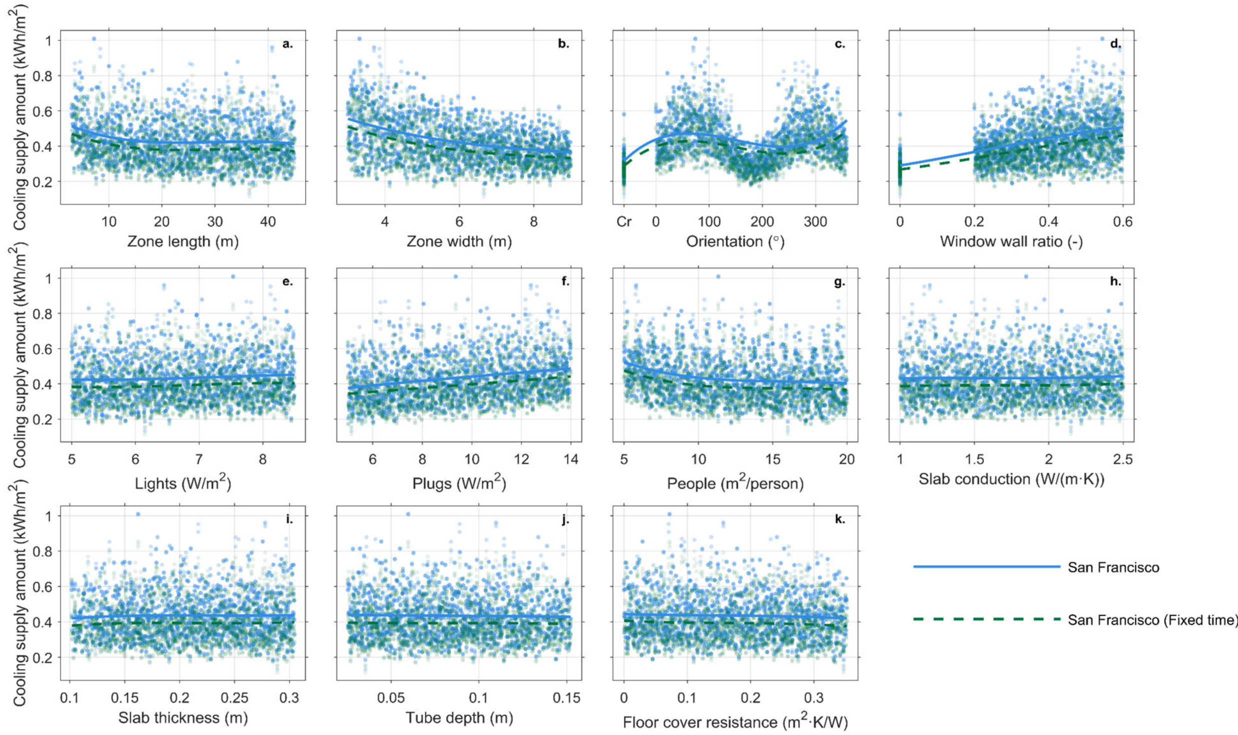

Fig. B2. Variation in cooling supply amount with parameters under fixed vs. flexible scheduling for ceiling ESS.

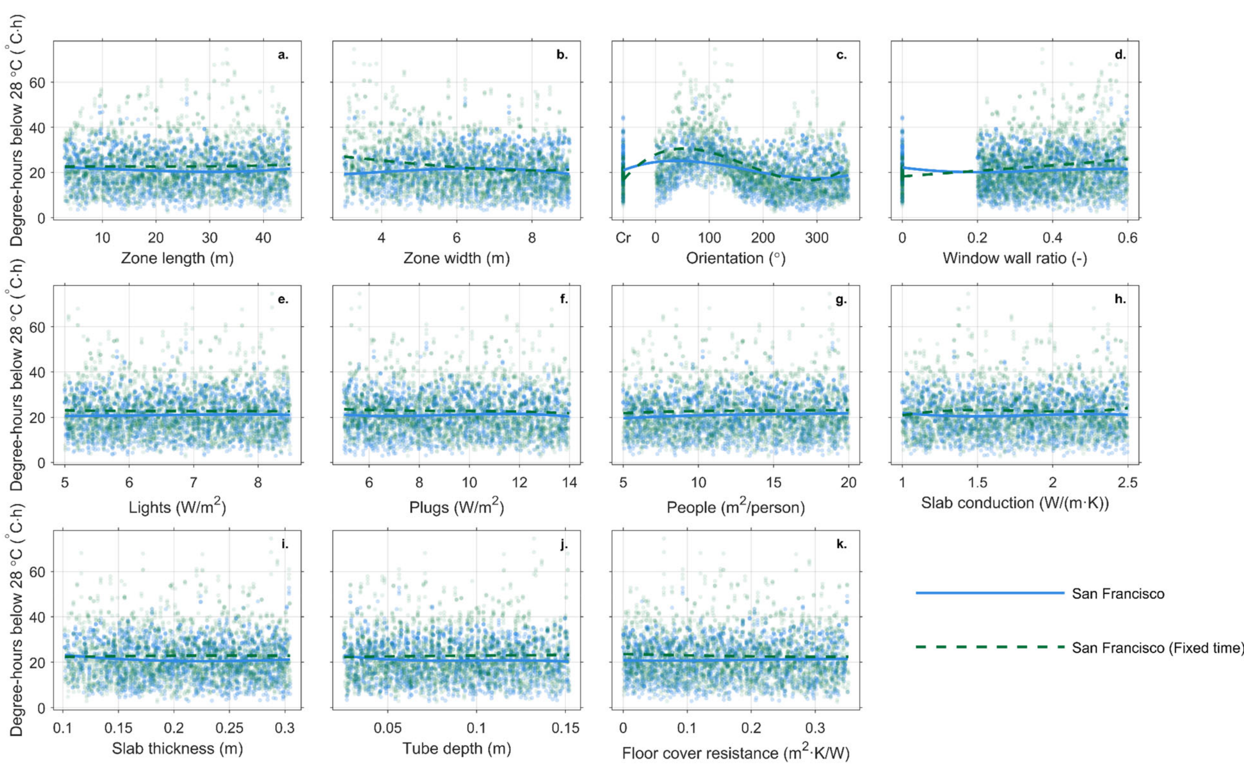

Fig. B3. Variation in degree-hours below 28 °C with parameters under fixed vs. flexible scheduling for ceiling ESS.

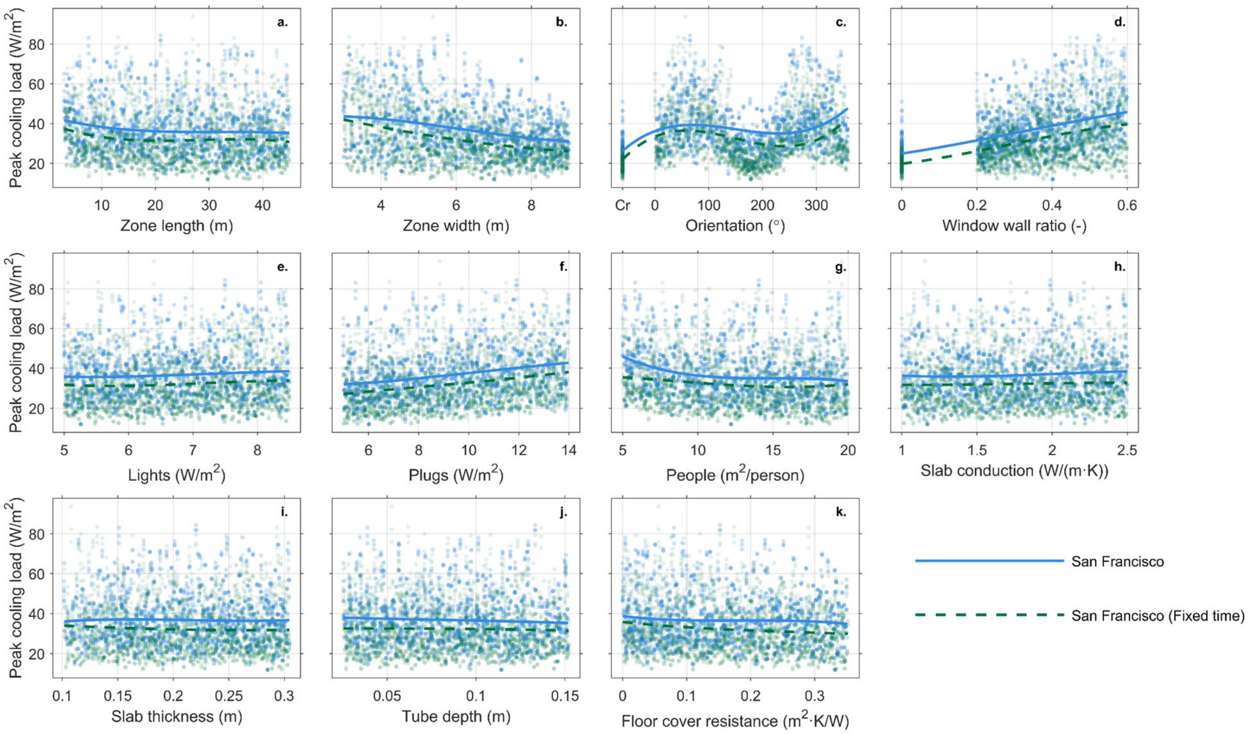

Fig. B4. Variation in peak cooling load with parameters under fixed vs. flexible scheduling for ceiling ESS.

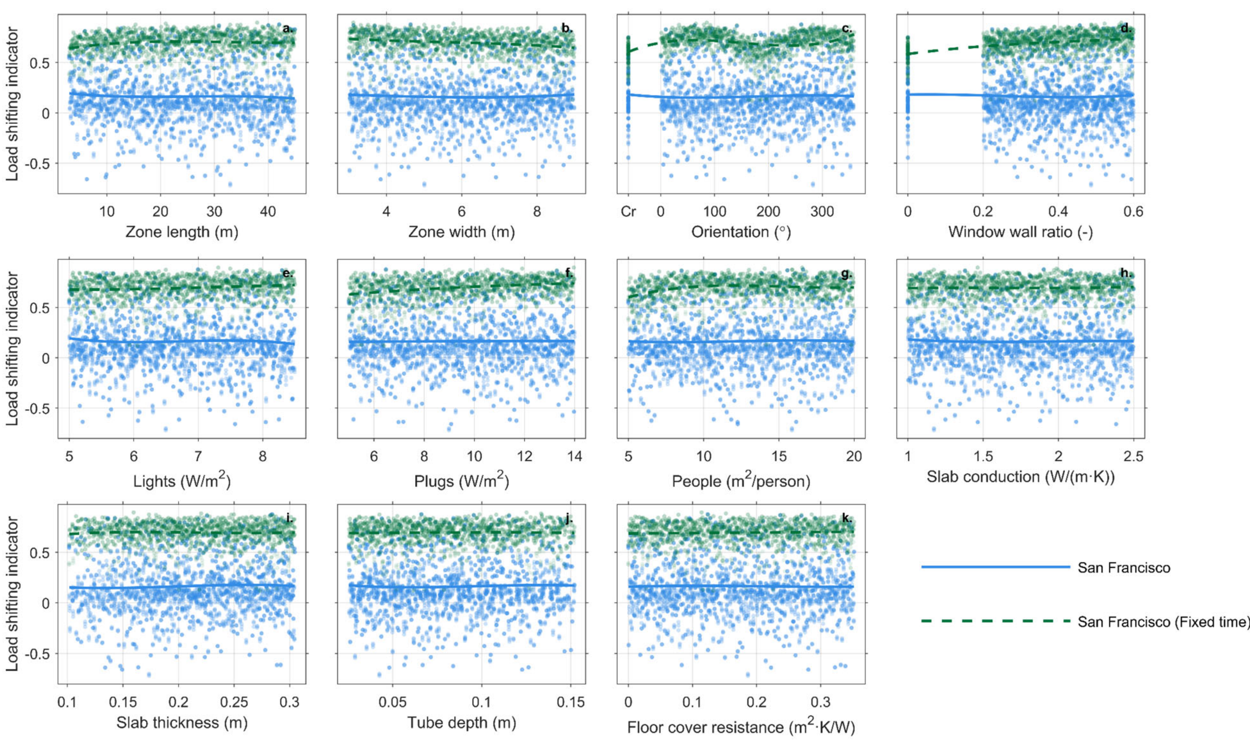

Fig. B5. Variation in load shifting indicator with parameters under fixed vs. flexible scheduling for ceiling TABS.

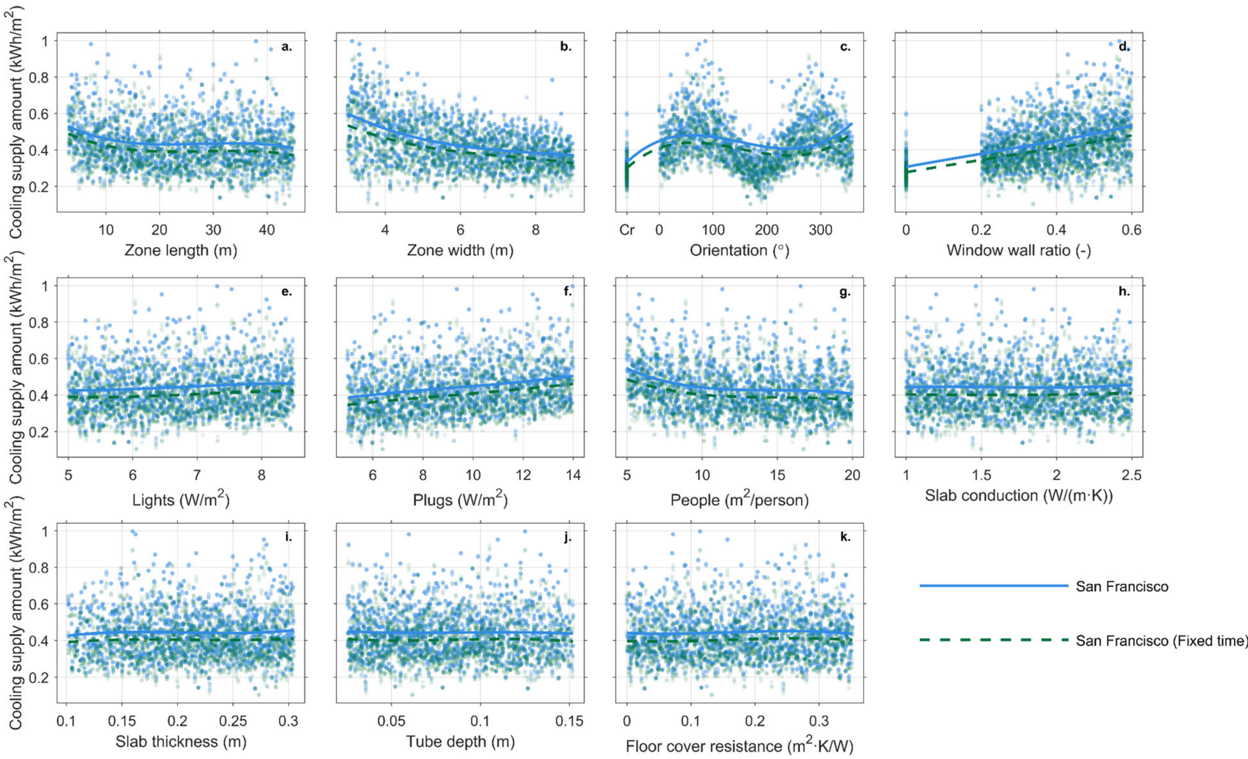

Fig. B6. Variation in cooling supply amount with parameters under fixed vs. flexible scheduling for ceiling TABS.

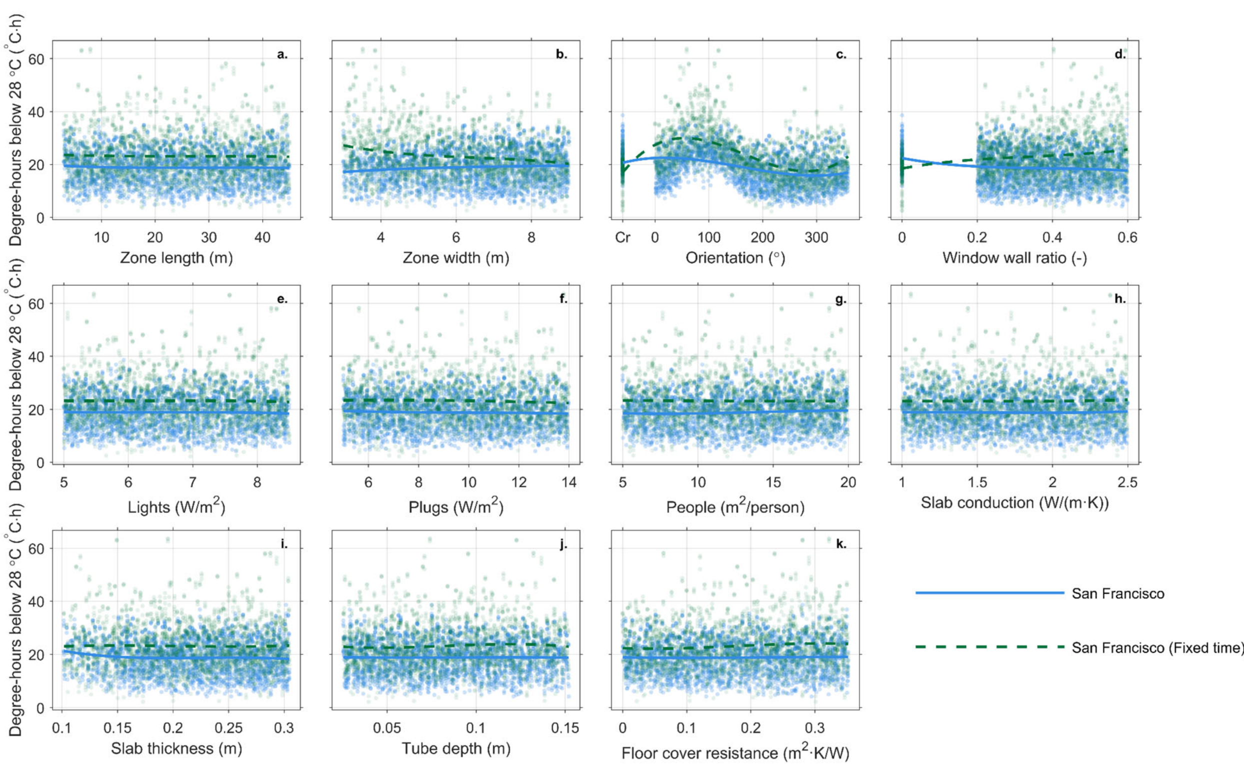

Fig. B7. Variation in degree-hours below 28 °C with parameters under fixed vs. flexible scheduling for ceiling TABS.

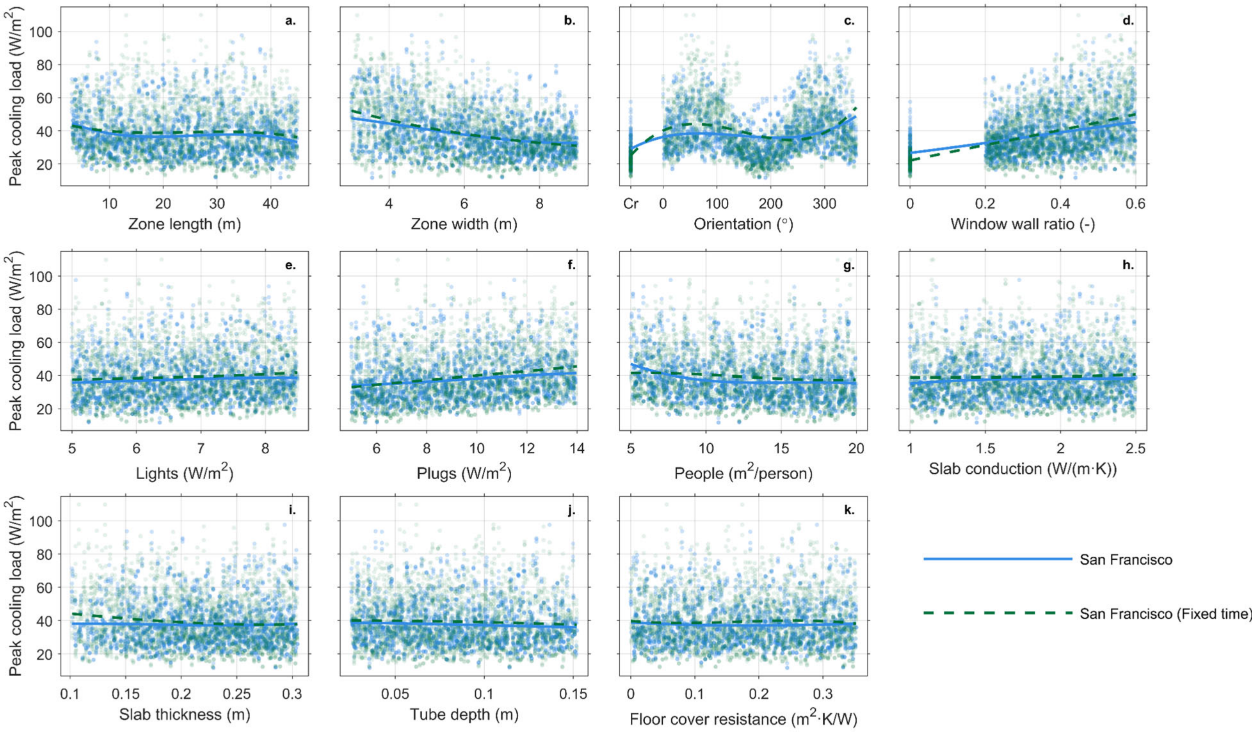

Fig. B8. Variation in peak cooling load with parameters under fixed vs. flexible scheduling for ceiling TABS.

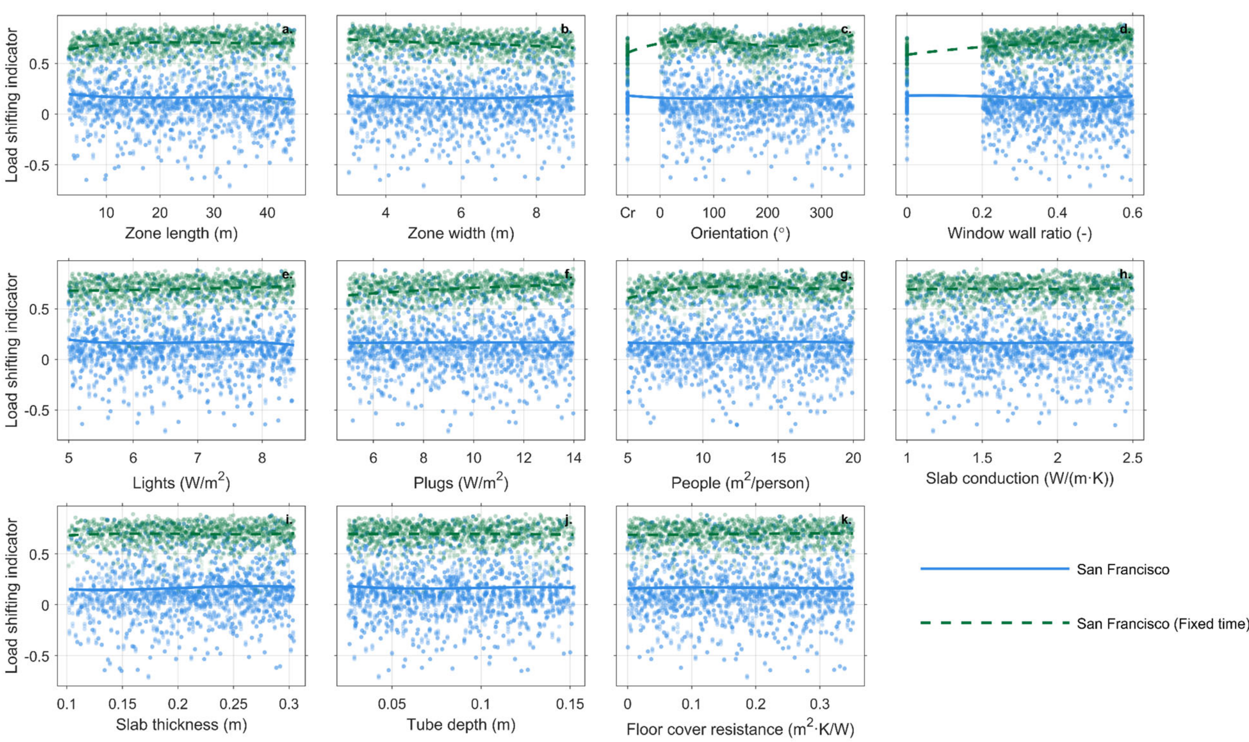

Fig. B9. Variation in load shifting indicator with parameters under fixed vs. flexible scheduling for floor TABS.

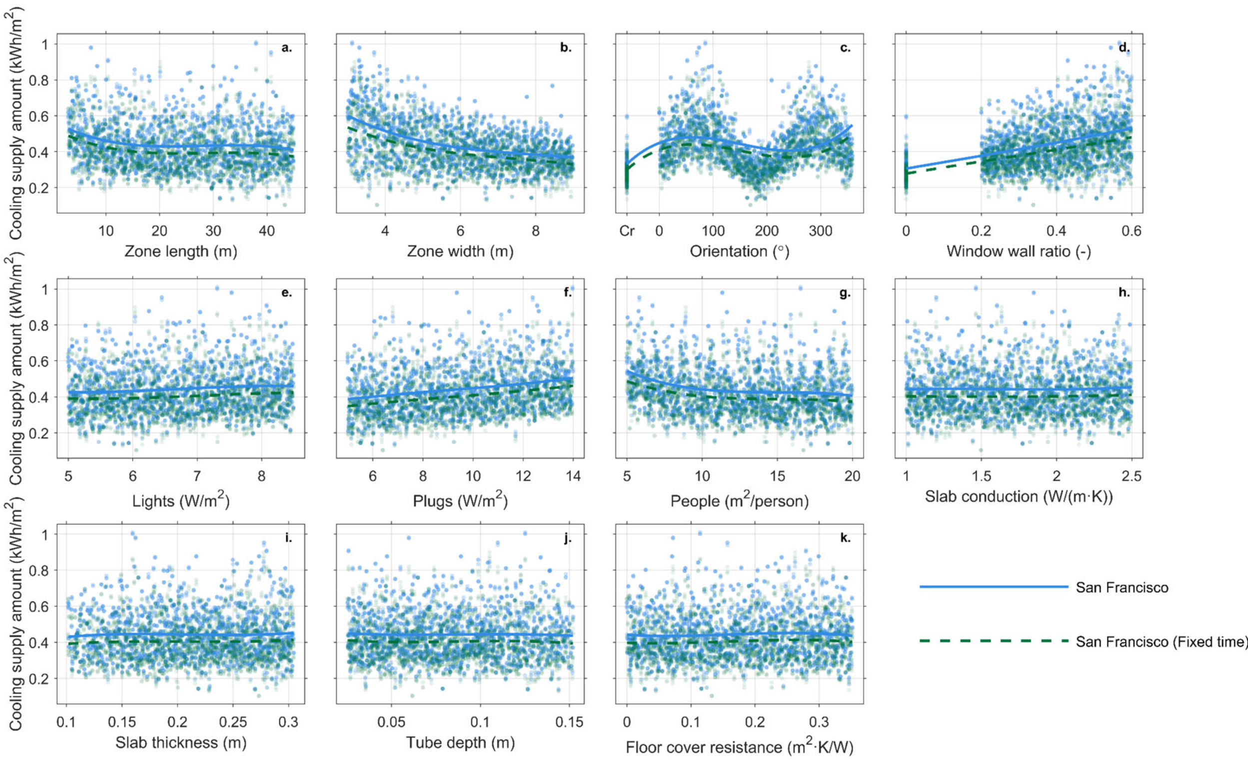

Fig. B10. Variation in cooling supply amount with parameters under fixed vs. flexible scheduling for floor TABS.

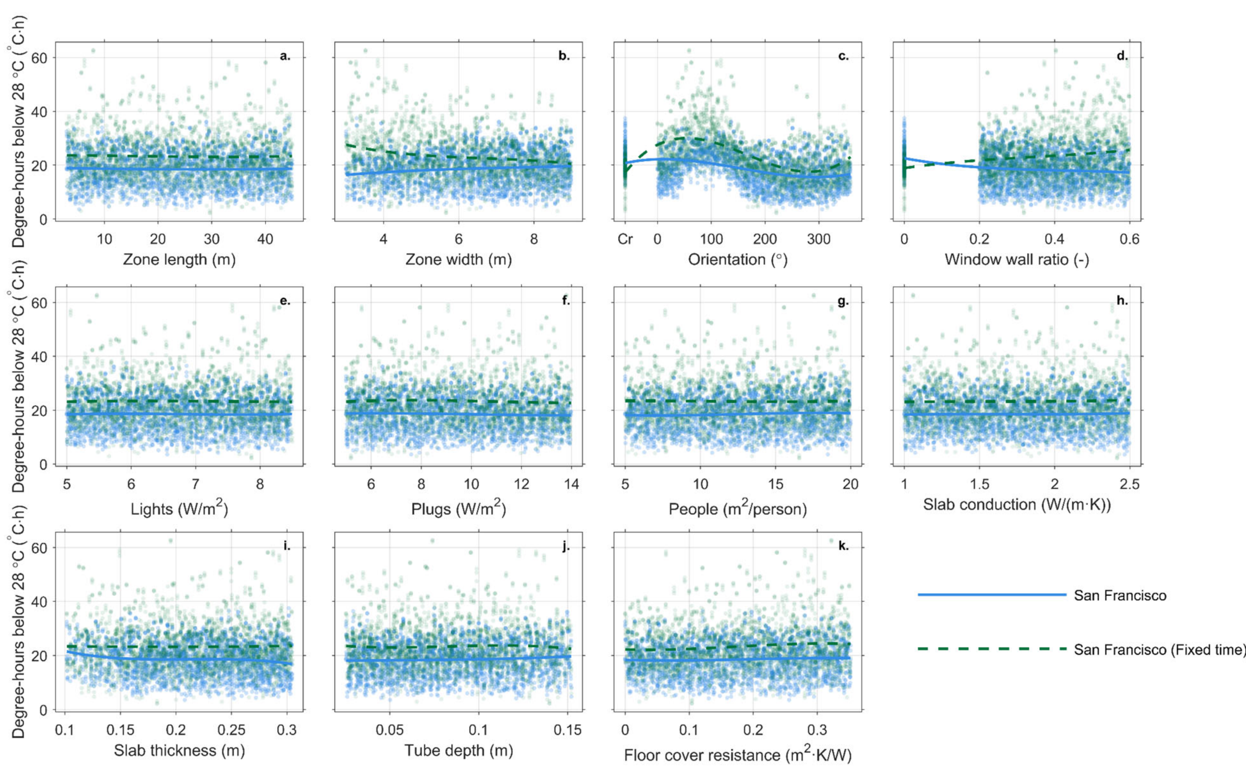

Fig. B11. Variation in degree-hours below 28 °C with parameters under fixed vs. flexible scheduling for floor TABS.

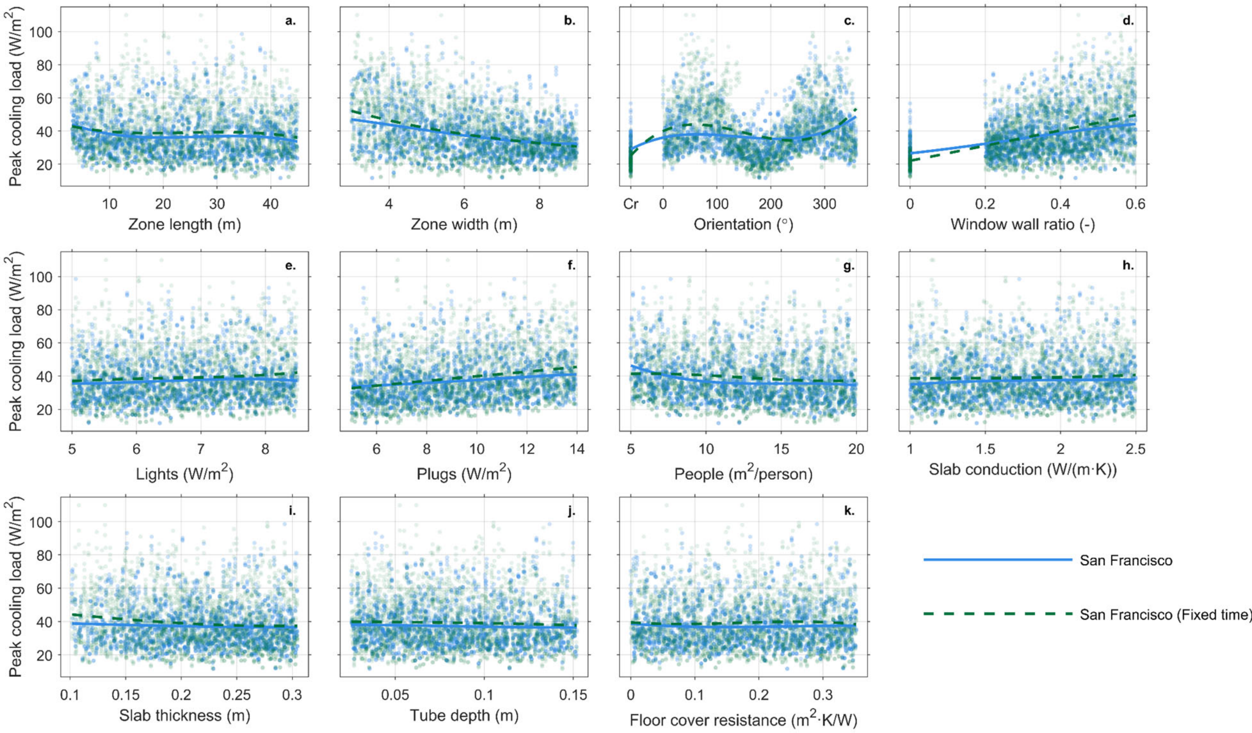

Fig. B12. Variation in peak cooling load with parameters under fixed vs. flexible scheduling for floor TABS.